Benzyl Functionalized Chiral 2^0 and 3^0 Amines: Synthesis, Characterization, Crystallographic and *In-silico* study

Abstract

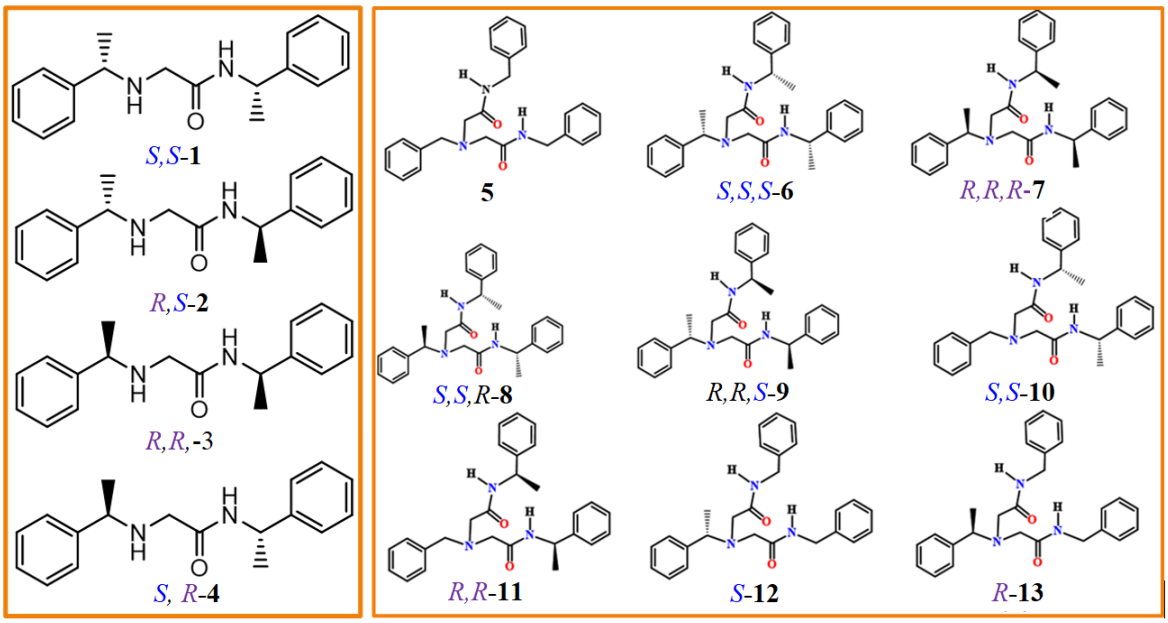

Selectively, a new series of organic chiral secondary amines viz. (*S*,*S*)-2-(1-phenylethylamino)-*N*-(1-phenylethyl)acetamide (*S*,*S*-**1**), (*R*,*S*)-2-(1-phenylethylamino)-N-(1-phenylethyl)acetamide (*R*,*S*-**2**), (*R*,*R*)-2-(1-phenylethylamino)-N-(1-phenylethyl)acetamide (*R*,*R*-**3**) and (*S*,R)-2-(1-phenylethylamino)-N-(1-phenylethyl)acetamide (*S*,*R*-**4**) and tertiary amines 2,2'-(benzylazanediyl)bis(*N*-benzylacetamide) **5**, 2,2'-(((*S*)-1-phenylethyl)azanediyl)bis(*N*-((*S*)-1-phenylethyl)acetamide) *S*,*S*,*S*-**6**, 2,2'-((*R*)-1-phenylethyl)azanediyl)bis(*N*-((*R*)-1-phenylethyl)acetamide) *R*,*R*,*R*-**7**, 2,2'-(((*R*)-1-phenylethyl)azanediyl)bis(*N*-((*S*)-1-phenylethyl)acetamide) *S*,*S*,*R*-**8**, 2,2'-(((*S*)-1-phenylethyl)azanediyl)bis(*N*-((*R*)-1-phenylethyl)acetamide) *R*,*R*,*S*-**9**, 2,2'-(benzylazanediyl)bis(*N*-((*S*)-1-phenylethyl)acetamide) *S*,*S*-**10**, 2,2'(benzylazanediyl)bis(*N*-((*R*)-1-phenylethyl)acetamide) *R*,*R*-**11**, (*S*)-2,2'-((1-phenylethyl)azanediyl)bis(*N*-benzylacetamide) *S*-**12** and (*R*)-2,2'-((1-phenylethyl)azanediyl)bis(*N*-benzylacetamide) *R*-**13** have been synthesized conveniently by an optimized reaction condition illustrated in Scheme 1. All the compounds have been characterized by elemental analysis and by using several spectroscopic techniques viz. ^{1}H and ^{13}C NMR, FTIR, UV-visible. Further, a DFT level calculations have been performed to reinforce the experimental data. The unprecedented molecular structures of some of the compounds have been determined by means of single

crystal X-ray diffraction (SCXRD) study. The chirality influence on the supramolecular packing of the molecules has been observed. For instance, molecules holding *S*-chirality viz. *S,S,S*-**6** and *S,S*-**10** form a fascinating 1D helical (P-type) supramolecular structure with a helical pitch of ~12.3 Å while molecules holding *R*-chirality viz. *R,R,R*-**10** and *R,R*-**11** form 1D helical (M-type) supramolecular structure with helical pitch of ~12.3 Å. Both the assemblies are sustained by several NH…O (2.9 Å, intermolecular) and NH…O (~2.1 Å, intra-molecular) donor-acceptor H-bonding contacts. Further, theorical calculation have been caried out to support the experimental data.

5.1 Introduction

Chirality plays an important role in various chemical fields that deal with biologically active molecules, in particular drug discovery, agrochemical development, food additive research, fragrance development, chiral pollutant detection.[1] Thus, chirality has become an important tool in modern drug development. The therapeutic activity of the enantiomers can differ severely in terms of toxicity and pharmacokinetics. [2] For example, oxaliplatin contains a chiral ligand (R, R)-cyclohexane-1,2-diamine showed more biological activity and chemical reactivity than its enantiomer containing the ligand (S, S)-cyclohexane-1, 2-diamine.[3] There is a growing interest in the research on chiral metal-based compounds for anticancer application. [4] Enantiomerically pure ferrocene–amino acid derivative showing a pronounced anticancer activity against leukemia and lymphoma cancer cell lines which has overcome multiple drug resistance has been reported recently. [5]

Very recently, chirality-related influence of optically pure enantiomeric pair *viz.* ferrocene functionalized chiral tertiary amines S,S-(-)-**1** and R,R-(+)-**2** on their anti-proliferative activity has been observed by us[6] wherein R,R-(+)-**2** exhibited more than 10 folds better antiproliferation (IC_{50}: 6.35±0.19 μM) than other enantiomer S,S-(-)-**1 (**IC_{50}: 65.96±0.12 μM**)** and four folds better activity than highly successful anticancer drug, cisplatin (IC_{50}: 24.3±1.7 μM) against HepG2 cell line. Moreover, apoptotic regulatory influence of various substituents of amidic nitrogen of ferrocene functionalized tertiary amines on TNFα inhibition has been investigated in detail.[7]

Besides, organocatalysts have attracted great deal of attention because of their significant advantages that includes environmentally benign and nontoxic nature, low cost of production, and even more importantly easy structural modifications to match specific requirement.[8] The key factors involved in the development of organocatalyst used in different organic transformation includes ability of catalyst to act as hydrogen bond donor or

one or more suitable chiral centers with requisite steric and electronic environment to affect the reaction rate and the stereo induction.[9]

In particular, chiral amines play an important role as the building blocks of many life-saving drugs and other industrially important chemicals that includes agrochemicals.[10] Literature revealed that around 40% of the currently used pharmaceuticals contain chiral amine functional groups in their structure.[11] Moreover, chiral secondary amine has a broad scope to be utilized in synthesis of dithiocarbamate ligand and their several transition/ non-transition metal complexes.[12] The dithiocarbamate group is considered as an important pharmacophore and it is used in the compounds of biological interest.[13]

These observations have encouraged us to design and synthesize a new series of optically pure enantiomers *viz.* chiral secondary amines *S,S*-**1,** *R,S*-**2,** *R,R*-**3**, S,*R*-**4** and chiral secondary amines **5,** *S,S,S*-**6,** *R,R,R*-**7,** *S,S,R*-**8,** *R,R,S*-**9,** *S,S*-**10,** *R,R*-**11,** *S*-**12** and *R*-**13** holding variable chirality in the ligand skeleton. The chiral secondary amines were synthesized, in particular, to derivatize them further into corresponding dithiocarbamate ligands and their ensuing transition-/ non-transition metal complexes. All the compounds were satisfactorily characterized by elemental analysis and by using several spectroscopic techniques. Further, a DFT level calculations have been performed to reinforce the experimental data. Single crystal X-ray diffraction (SCXRD) technique has been utilized to determine the unprecedented molecular structures of some of the representative compounds and to study the influence of chirality on their crystal packing patterns.

5.2 Experimental

5.2.1 Materials and measurements

All solvents were purchased from the commercial sources and were freshly distilled prior to use. All the reagents such as benzyl amine, (*R*)-1-(naphthalen-1-yl) ethan-1-amine and (*S*)-1-(naphthalen-1-yl)ethan-1-amine) were purchased from TCI Chemicals Limited, these were used without further purification. Elemental analyses (C, H, N) were carried out on a Perkin-Elmer 2400 analysers. Thin Layer Chromatography was performed on Merck 60 F254 Aluminium coated plates. FT-IR spectra were recorded in the 4000-400 cm^{-1} range using a Perkin-Elmer FT-IR spectrometer as KBr pellets. The ^{1}H and ^{13}C NMR spectra of relevant compounds were obtained on a Bruker AV-III 400 MHz spectrometer in spectrometer with $CDCl_3$ as solvent and TMS as internal standard. UV-visible spectra were recorded on a JASCO V-730 UV-visible spectrophotometer.

5.2.2 General procedure for the synthesis of *S,S*-1, *R,S*-2, *R,R*-3 and S,*R*-4

(*S*/*R*) -2- iodo-N-(1-phenylethyl)acetamide (289mg, 1mmol) were added portion wise to the solution of acetonitrile solution containing (*S*/*R*)-1-phenylethan-1-amine (127 µl, 1 mmol) and Na_2CO_3 (318mg, 3mmol). The reaction mixture was reflux for 5 hours at 60 ^{0}C temperature. The progress of the reaction was monitored by thin layer chromatography and ninhydrin. The reaction mixture was cooled at room temperature and solvent was removed under vacuum. Distilled water was added in the solid residue and the crude product was extracted by using dichloromethane. It was dried over Na_2SO_4 for 4 hours and the solvent was removed by rotator evaporator. The residue was column chromatographed to give pale white thick oily liquid products (*S,S*)-2-(1-phenylethylamino)-*N*-(1-phenylethyl)acetamide (*S,S*-**1**), (*R,S*)-2-(1-phenylethylamino)-N-(1-phenylethyl)acetamide (*R,S*-**2**), (*R,R*)-2-(1-phenylethylamino)-N-(1-phenylethyl)acetamide (*R,R*-**3**) and (*S*,R)-2-(1-phenylethylamino)-N-(1-phenylethyl)acetamide (*S,R*- **4**) in 85-87 % yield.

5.2.3 General procedure for the synthesis of 5, *S,S,S*-6, *R,R,R*-7, *S,S,R*-8, *R,R,S*-9, *S,S*-10, *R,R*-11, *S*-12 and *R*-13

N-benzyl-2-iodoacetamide, (*S*)-2-iodo-N-(1-phenylethyl)acetamide and (*R*)-2-iodo-N-(1-phenylethyl)acetamide were prepared by reacting corresponding α-chloro derivatives with KI in acetone and it was subsequently utilized in the synthesis of corresponding amide functionalized tertiary amines **5-13** (Scheme 1), *ca* N-benzyl-2-iodoacetamide (500mg, 2mmol), (S)-2-iodo-N-(1-phenylethyl)acetamide (578mg, 2mmol) or (R)-2-iodo-N-(1-phenylethyl)acetamide (578mg, 2mmol) was added portion wise to the acetonitrile solution (30-40 ml) of benzyl amine (109 µl, 1 mmol), (S)-1-phenylethan-1-amine(127 µl, 1 mmol) or (R)-1-phenylethan-1-amine (127 µl, 1 mmol) containing Na_2CO_3 (318mg, 3mmol). The reaction mixture was reflux for 6 hrs and the progress of the reaction was monitored by ninhydrin on thin layer chromatography. The reaction mixture was cooled at room temperature and solvent was removed under vacuum. Distilled water was added in the solid residue and the crude product was extracted by using dichloromethane. It was dried over Na_2SO_4 for 4 hrs and the solvent was removed by rotator evaporator. The residue was column chromatographed to yield the products 2,2'-(benzylazanediyl)bis(*N*-benzylacetamide) **5**, 2,2'-(((*S*)-1-phenylethyl)azanediyl)bis(*N*-((*S*)-1-phenylethyl)acetamide) *S,S,S*-**6**, 2,2'-((*R*)-1-phenylethyl)azanediyl)bis(*N*-((*R*)-1-phenylethyl)acetamide) *R,R,R*-**7**, 2,2'-(((*R*)-1-phenylethyl)azanediyl)bis(*N*-((*S*)-1-phenylethyl)acetamide) *S,S,R*-**8**, 2,2'-(((*S*)-1-phenylethyl)azanediyl)bis(*N*-((*R*)-1-phenylethyl)acetamide) *R,R,S*-**9**, 2,2'-

(benzylazanediyl)bis(*N*-((*S*)-1-phenylethyl)acetamide) *S,S*-**10**, 2,2'(benzylazanediyl)bis(*N*-((*R*)-1-phenylethyl)acetamide) *R,R*-**11**, (*S*)-2,2'-((1-phenylethyl)azanediyl)bis(*N*-benzylacetamide) *S*-**12** and (*R*)-2,2'-((1-phenylethyl)azanediyl)bis(*N*-benzylacetamide) *R*-**13** in good yields 80-89 %.

5.2.4 X-ray crystallography and data collection

Crystals of 2,2'-(((*S*)-1-phenylethyl)azanediyl)bis(*N*-((*S*)-1-phenylethyl)acetamide) *S,S,S*-**6**, 2,2'-((*R*)-1-phenylethyl)azanediyl)bis(*N*-((*R*)-1-phenylethyl)acetamide) *R,R,R*-**7**, 2,2'-(benzylazanediyl)bis(*N*-((*S*)-1-phenylethyl)acetamide) *S,S*-**10** and 2,2'(benzylazanediyl)bis(*N*-((*R*)-1-phenylethyl)acetamide) *R,R*-**11** suitable for X-ray crystallographic study were obtained in ethyl acetate solution by slow evaporation at 4 °C. The intensity data were collected on Oxford diffraction X Calibur diffractometer equipped with Eos CCD detector at 293 K for [$C_{28}H_{33}N_3O_2$] (*S,S,S*-**6**), [$C_{28}H_{33}N_3O_2$] (*R,R,R*-**7**), [$C_{54}H_{62}N_6O_4$] (*S,S*-**10**) and [$C_{54}H_{62}N_6O_4$] (*R,R*-**11**) respectively. Monochromatic Mo-Kα X-ray (λ=0.71073 Å) was used for the measurements. Data were collected and reduced by using the ‘‘CrysAlispro’’ program.[14] An empirical absorption correction using spherical harmonics was implemented in ‘‘SCALE3 ABSPACK’’ scaling algorithm. The crystal structures were solved by direct methods using SHELXL-97 [15] and the refinement was carried out against F2 using SHELXL-97 program package.[16] All non-hydrogen atoms were refined anisotropically.

Table 1. Micro-, mass- and IR analysis data for compounds **1-13**.

Entry	Molecular Formula	Molecular Weight	Yield (%)	MP (°C)	Elemental Analysis % Found (calculated)			IR data (KBr disc) υ_{max}/cm^{-1}
					C	H	N	
S,S-**1**	$C_{18}H_{22}N_2O$	282	87	-				3272(N-H), 3007(C-H), 2975(C-H), 1651(C=O), 1537, 1452, 1216, 1130, 758, 700.
R,S-**2**	$C_{18}H_{22}N_2O$	282	86	-				3309(N-H). 2971(C-H), 2927(C-H), 1656(C=O), 1518, 1451, 1217, 1127, 753, 700.
R,R-**3**	$C_{18}H_{22}N_2O$	282	85	-				3243(N-H), 2973(C-H), 2930(C-H), 1660(C=O),1528, 1452, 1216, 1129, 758, 700.
S,*R*-**4**	$C_{18}H_{22}N_2O$	282	87	-				3283(N-H), 2974(C-H), 1654(C=O), 1524, 1451, 1219, 1127, 752, 700.
5	$C_{25}H_{27}N_3O_2$	401	80	96	74.59 (74.79)	6.15 (6.78)	10.56 (10.47)	3209 (N-H), 3028 (C-H), 2835 (C-H), 2603 (C-H), 1681 (C=O), 1531, 1392, 1269,1103, 1026, 894, 698, 659, 497, 482.
S,S,S-**6**	$C_{28}H_{33}N_3O_2$	443	83	152	75.62 (75.81)	7.62 (7.50)	9.56 (9.47)	3188 (N-H), 3052 (C-H), 2970 (C-H), 1665 (C=O), 1634 (C=O), 1548, 1370, 1208, 1133, 1021, 761, 739, 699, 538.
R,R,R-**7**	$C_{28}H_{33}N_3O_2$	443	82	152	75.67 (75.81)	7.59 (7.50)	9.64 (9.47)	3191 (N-H), 3053 (C-H), 2969 (C-H), 2927 (C-H), 1665 (C=O), 1637 (C=O), 1549, 1449, 1371, 1238, 1178, 1021, 761, 700.
S,S,R-**8**	$C_{28}H_{33}N_3O_2$	443	86	110	75.83 (75.81)	7.56 (7.50)	9.54 (9.47)	3237 (N-H), 3058 (C-H), 2971 (C-H), 1662 (C=O), 1637 (C=O), 1549, 1375, 1264, 1132, 767, 700, 616.
R,R,S-**9**	$C_{28}H_{33}N_3O_2$	443	80	110	75.82 (75.81)	7.48 (7.50)	9.46 (9.47)	3234 (N-H), 3054 (C-H), 2971 (C-H), 1662 (C=O), 1637 (C=O), 1548, 1451, 1372, 1243, 771, 700.
S,S-**10**	$C_{27}H_{31}N_3O_2$	429	82	126	75.51 (74.49)	7.31 (7.27)	9.75 (9.78)	3193 (N-H), 3034 (C-H), 2973 (C-H), 2930 (C-H), 2870 (C-H), 1662 (C=O), 1640 (C=O), 1549, 1270, 1133, 748, 699.
R,R-**11**	$C_{27}H_{31}N_3O_2$	429	84	126	75.50 (74.49)	7.32 (7.27)	9.76 (9.78)	3192 (N-H), 3033 (C-H), 2973 (C-H), 1662 (C=O), 1639 (C=O), 1450, 1377, 1239, 1133, 1022, 746, 698.
S-**12**	$C_{26}H_{29}N_3O_2$	415	87	-	75.17 (75.15)	7.05 (7.03)	10.13 (10.11)	3290 (N-H), 3011 (C-H), 1653 (C=O), 1532, 1453, 1216, 771, 742, 701, 667.
R-**13**	$C_{26}H_{29}N_3O_2$	415	89		75.19 (75.15)	7.08 (7.03)	10.12 (10.11)	3284 (N-H), 3010 (C-H), 1651 (C=O), 1538, 1454, 1217, 1028, 771, 700 ,666.

Table 2. NMR spectral data for compounds **1-13**.

Entry	NMR Data (ppm)	
	^{1}H NMR ($CDCl_3$)	**^{13}C NMR ($CDCl_3$)**
S,S-**1**	8.18(s, 1H, N*H*CO); 7.20-7.34(m, 10*H*, Bz); 4.93(m, 1H, -C*H*); 3.67 (q, 1H, -C*H*); 2.96(S, 2H, -CH_2CO); 1.33(d, 3H, -CH_3); 1.16(d, 3H, -CH_3).	170.7, 145.0, 143.0 129.0, 128.7 127.5, 126.3, 60.9, 55.8, 48.3, 23.0.
R,S-**2**	7.53(s, 1H, N*H*CO); 7.23-7.33(m, 10*H*, Bz); 5.13(m, 1H, -C*H*); 3.75 (q, 1H, -C*H*); 3.24(S, 2H, -CH_2CO); 1.44(d, 3H, -CH_3); 1.39(d, 3H, -CH_3).	170.7, 145.0, 143.6 139.9, 128.9 127.1, 126.6, 57.8, 49.4, 47.9, 23.4.
R,R-**3**	8.17(s, 1H, N*H*CO); 7.21-7.27(m, 10*H*, Bz); 4.93(m, 1H, -C*H*); 3.64 (q, 1H, -C*H*); 2.96(S, 2H, -CH_2CO); 1.34(d, 3H, -CH_3); 1.16(d, 3H, -CH_3).	170.7, 145.0, 143.0 139.8,129.2, 128.7, 127.2, 126.4, 57.6, 48.2 23.1, 21.3.
S,*R*-**4**	8.24(s, 1H, N*H*CO); 7.22-7.33(m, 10*H*, Bz); 4.97(m, 1H, -C*H*); 3.68 (q, 1H, -C*H*); 3.01(S, 2H, -CH_2CO); 1.36(d, 3H, -CH_3); 1.27(d, 3H, -CH_3).	170.4, 145.7, 145.0, 128.7, 128.7, 127.2, 127.1, 126.3, 57.7, 50.4, 48.1, 24.6, 22.8.
5	7.19-7.33 (m, 15H, *Ph*); 4.37-4.39 (s, 4H, -CH_2NH); 3.68 (s, 2H, -CH_2Ph); (δ ppm) 3.20 (s, 4H, -CH_2N).	170.3, 138.1, 137.0, 129.0, 128.7, 128.6, 127.8, 127.6, 127.4, 59.7, 58.2, 43.2.
S,S,S-**6**	7.50 (s, 1H, N*H*CO); 7.48 (s, 1H, N*H*CO); 7.22-7.34 (m, 15*H*, *Ph*); 5.10 (m, 2H, -C*H*); 3.90 (q, 1H, -C*H*); 3.2 (d, 2H, -CH_2CO); 3.10 (d, 2H, -CH_2CO); 1.48 (d, 6H, -CH_3); 1.35 (d, 3H, - CH_3).	170.2, 143.3, 142.1, 128.6, 128.5, 127.5, 127.5, 127.2, 126.1, 60.9, 55.9, 48.7, 22.1, 16.8.
R,R,R-**7**	7.21-7.34 (m, 15H, *Ph*); 5.11(m, 2H, -C*H*); 3.86 (q, 1H, -C*H*); 3.24 (d, 2H, -CH_2CO); 3.1 (d, 2H, -CH_2CO); 1.48 (d, 6H, -CH_3); 1.35 (d, 3H, -CH_3).	170.2, 143.4, 142.1, 128.6, 128.5, 127.5, 127.5, 127.2, 126.1, 60.9, 55.9, 48.7, 22.1, 16.8.
S,S,R-**8**	7.23-7.34(m, 15H, *Ph*); 5.09(m, 2H, -C*H*); 3.88(q, 1H, -C*H*); 3.24(d, 2H, -CH_2CO); 3.12(d, 2H, -CH_2CO); 1.48(d, 6H, -CH_3); 1.36(d, 3H, -CH_3).	170.2, 143.4, 142.2, 128.6, 128.6, 128.5, 127.5, 127.5, 127.4, 127.2, 126.5, 126.1, 126.0, 60.8, 58.5, 55.9, 50.4, 48.7, 48.2, 23.7, 22.1, 22.0,16.5.
R,R,S-**9**	7.23-7.34(m, 15H, *Ph*); 5.09(m, 2H, -C*H*); 3.88(q, 1H, -C*H*); 3.24(d, 2H, -CH_2CO); 3.12(d, 2H, -CH_2CO); 1.48(d, 6H, -CH_3); 1.36(d, 3H, -CH_3).	170.2, 143.2, 142.2, 128.7, 128.6, 128.5, 127.5, 127.4, 127.2, 127.2, 126.6, 126.1, 126.0, 60.8, 55.9, 48.7, 48.2, 22.1, 22.0, 16.5.
S,S-**10**	7.12-7.33(m, 15H, *Ph*); 5.09(m, 2H, -C*H*); 3.67 (s, 2H, -CH_2); 3.18(s, 4H, -CH_2CO); 1.43(d, 6H, -CH_3).	169.2, 143.1, 137.1, 129.0, 128.7, 128.7, 127.6, 127.4, 126.1, 59.6, 58.3, 48.6, 21.9.
R,R-**11**	7.09-7.34(m, 15H, *Ph*); 5.09(m, 2H, -C*H*); 3.67 (s, 2H, -CH_2); 3.18(s, 2 4H, -CH_2CO); 1.44(d, 6H, -CH_3).	169.2, 143.1, 137.1, 129.0, 128.7, 128.6, 127.8, 127.4, 126.1, 59.6, 58.3, 48.6, 21.9.
S-**12**	8.208(s, 2H, -N*H*CO); 7.18-7.35(m, 15H, *Ph*); 4.35(d, 4H, CH_2NH); 3.69(q, 1H, -C*H*); 3.18(d, 2H, -CH_2CO); 3.06(d, 2H, -CH_2CO); 1.32(dd, 3H, CH_3).	171.1, 141.9, 138.2, 128.7, 128.6, 128.5, 127.6, 127.6, 127.5, 127.5, 127.5, 127.4, 126.5, 61.1, 56.0, 43.3, 17.0.
R-**13**	8.08(s, 2H, -N*H*CO); 7.24-7.66(m, 15H, *Ph*); 4.42(d, 4H, CH_2NH); 3.75(q, 1H, -C*H*); 3.20(s, 4H, -CH_2CO); 1.37(d, 3H, CH_3).	171.3, 141.9, 138.2, 128.6, 128.5, 127.6, 127.5, 127.5, 127.3, 61.1, 55.9, 43.2, 17.0.

5.3 RESULTS AND DISCUSSION

5.3.1 Synthesis and Characterization.

A typical reaction involving primary amine viz benzyl amine, (*R*)-1-phenylethan-1-amine and (*S*)-1-phenylethan-1-amine, affords access to a new series of chiral secondary amines viz. N-((*S*)-1-phenylethyl)-2-(((*S*)-1-phenylethyl)amino)acetamide (*S,S*-**1**), N-((*S*)-1-phenylethyl)-2-(((*R*)-1-phenylethyl)amino)acetamide (*R*,S-**2**), N-((*R*)-1-phenylethyl)-2-(((*R*)-1-phenylethyl)amino)acetamide (*R,R*-**3**) and N-((*R*)-1-phenylethyl)-2-(((S)-1-phenylethyl)amino)acetamide (*S*, R-**4**) and chiral/achiral tertiary amines viz 2,2'-(benzylazanediyl)bis(*N*-benzylacetamide) **5**, 2,2'-(((*S*)-1-phenylethyl)azanediyl)bis(*N*-((*S*)-1-phenylethyl)acetamide) *S,S,S*-**6**, 2,2'-((*R*)-1-phenylethyl)azanediyl)bis(*N*-((*R*)-1-phenylethyl)acetamide) *R,R,R*-**7**, 2,2'-(((*R*)-1-phenylethyl)azanediyl)bis(*N*-((*S*)-1-phenylethyl)acetamide) *S,S,R*-**8**, 2,2'-(((*S*)-1-phenylethyl)azanediyl)bis(*N*-((*R*)-1-phenylethyl)acetamide) *R,R,S*-**9**, 2,2'-(benzylazanediyl)bis(*N*-((*S*)-1-phenylethyl)acetamide) *S,S*-**10**, 2,2'(benzylazanediyl)bis(*N*-((*R*)-1-phenylethyl)acetamide) *R,R*-**11**, (*S*)-2,2'-((1-phenylethyl)azanediyl)bis(*N*-benzylacetamide) *S*-**12** and (*R*)-2,2'-((1-phenylethyl)azanediyl)bis(*N*-benzylacetamide) *R*-**13** as per the **Scheme 1.** After workup the products were obtained as thick liquid and white powder for secondary and tertiary respectively in 80−89% isolated yields. All the compounds **(1-13)** have been characterized thoroughly by microanalysis, standard spectroscopy technique. The spectroscopic analysis data, such as IR, NMR and UV-visible spectra of the compounds **(1-13)** are consistent with their chemical formula determined by elemental analysis. The molecular structures of 2,2'-(((*S*)-1-phenylethyl)azanediyl)bis(*N*-((*S*)-1-phenylethyl)acetamide) *S,S,S*-**6**, 2,2'-((*R*)-1-phenylethyl)azanediyl)bis(*N*-((*R*)-1-phenylethyl)acetamide) *R,R,R*-**7**, 2,2'-(benzylazanediyl)bis(*N*-((*S*)-1-phenylethyl)acetamide) *S,S*-**10** and 2,2'(benzylazanediyl)bis(*N*-((*R*)-1-phenylethyl)acetamide) *R,R*-**11** were further confirmed by single crystal X-ray diffraction study.

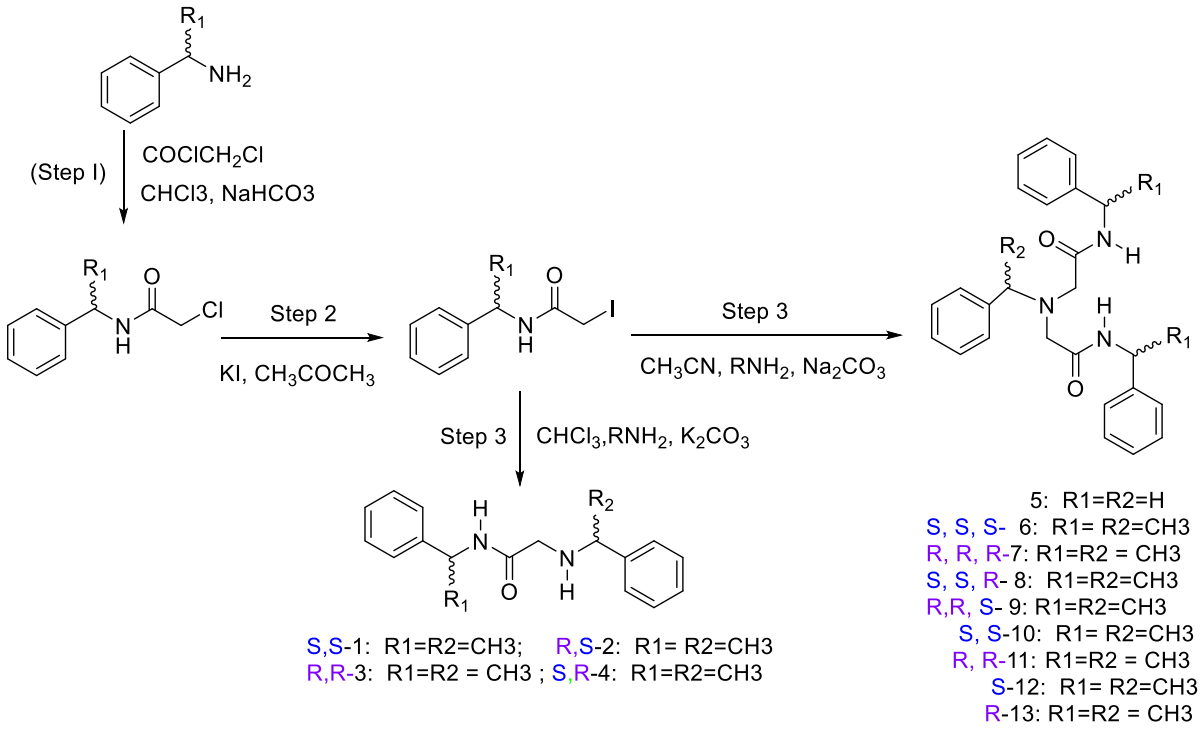

Scheme 1. General synthetic strategies adopted for chiral secondary amines or chiral/achiral tertiary amines.

All the compounds are fairly soluble in common organic solvents and found to be stable in pure state and in the solution over a period of days. The compositions and phase purity of the samples were confirmed by microanalysis and by ^{1}H and ^{13}C spectroscopy. The NMR (Annexure 1-26) and IR spectra gives confirmation of various groups viz. alkyl, amino-amido- and aryl present in **1-13**. The assigned IR and NMR data are summarized in the experimental section. (Table 1, Table 2) Methylene protons appear in the range of 3.67-3.90 ppm and 4.93-5.13 ppm and amidic proton appear at ~8 ppm in the ^{1}H NMR spectrum of **1-13.** Notably, di-amide functionalized 3º amines (5-13) show two different CO stretching frequencies in 1665-1634 cm^{-1} region (Annexures 27-39) due to the involvement of one of the amidic CO in intermolecular hydrogen bonding as revealed by X-ray diffraction study (vide infra) and in case of mone-amide functionalized 2º amine gives only one CO stretching frequencies in ~1650 cm^{-1} region.

The UV-visible absorption spectral data of **1-13** were recorded in 10^{-5} M CH_3CN solution are given in Table 3. The electronic absorption spectrum of all compound gives shorter absorbance band (250-260 nm) region **(**Figure 1) which is mainly attributed to the locally excited intra-ligand $\pi \rightarrow \pi^*$transitions. In case of tertiary amines, UV-Visible spectra gave three $\pi \rightarrow \pi^*$ transitions absorption bands apparently due to three different types of π

bond. The λ_{max} valve for compounds **5-13** appears at ~260 nm due to $\pi \rightarrow \pi^*$ transition and remain unaffected by the polyaromatic substituents present on compounds.

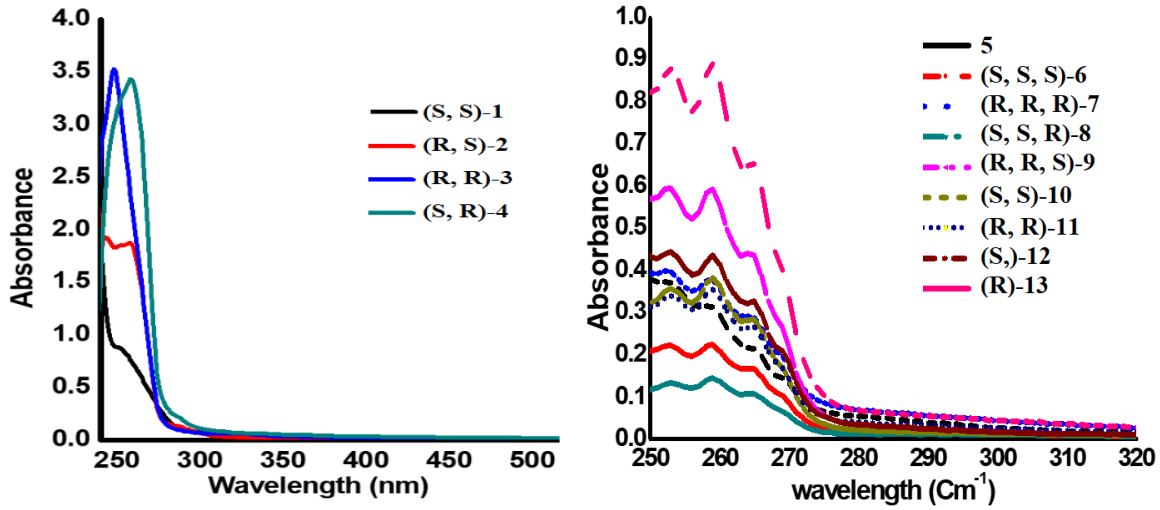

(a) **(b)**

Figure 1. (a) Absorbance spectra of Compounds *S,S*-**1,** *R,S*-**2,** *R,R*-**3** and S,*R*-**4** in 10^{-5} M CH_3CN; (b) Absorbance spectra of Compounds **5,** *S,S,S*-**6,** *R,R,R*-**7,** *S,S,R*-**8,** *R,R,S*-**9,** *S,S*-**10,** *R,R*-**11,** *S*-**12** and *R*-**13** in 10^{-5} M CH_3CN.

Table 3. UV-visible spectral data of compounds in 10^{-5} M CH_3CN

Entry	λ_{max} nm (10^{-4}M, ε L Mol^{-1} cm^{-1})
S,S-**1**	255 (10850) $\pi \rightarrow \pi^*$
R,S-**2**	259 (18429) $\pi \rightarrow \pi^*$
R,R-**3**	256 (34421) $\pi \rightarrow \pi^*$
S,*R*-**4**	267 (31834) $\pi \rightarrow \pi^*$
5	252 (3726) $\pi \rightarrow \pi^*$ benzene, 258 (3146) $\pi \rightarrow \pi^*$ amide 264 (2157) $\pi \rightarrow \pi^*$
S,S,S-**6**	252 (2224) $\pi \rightarrow \pi^*$ benzene, 259 (2249) $\pi \rightarrow \pi^*$ amide 265 (1683) $\pi \rightarrow \pi^*$
R,R,R-**7**	253 (3775) $\pi \rightarrow \pi^*$ benzene, 258 (3794) $\pi \rightarrow \pi^*$ amide 265 (2881) $\pi \rightarrow \pi^*$
S,S,R-**8**	252 (3404) $\pi \rightarrow \pi^*$ benzene, 259 (3543) $\pi \rightarrow \pi^*$ amide 264 (2655) $\pi \rightarrow \pi^*$
R,R,S-**9**	252 (5938) $\pi \rightarrow \pi^*$ benzene, 258 (5926) $\pi \rightarrow \pi^*$ amide 265 (2841) $\pi \rightarrow \pi^*$
S,S-**10**	252 (3566) $\pi \rightarrow \pi^*$ benzene,259 (3828) $\pi \rightarrow \pi^*$ amide 265 (2841) $\pi \rightarrow \pi^*$
R,R-**11**	252 (3526) $\pi \rightarrow \pi^*$ benzene, 256 (3626) $\pi \rightarrow \pi^*$ amide 264 (2826) $\pi \rightarrow \pi^*$
S-**12**	253 (4433) $\pi \rightarrow \pi^*$ benzene, 258 (4356) $\pi \rightarrow \pi^*$ amide 264 (3254) $\pi \rightarrow \pi^*$
R-**13**	252 (8779) $\pi \rightarrow \pi^*$ benzene, 258 (8881) $\pi \rightarrow \pi^*$ amide 264 (3535) $\pi \rightarrow \pi^*$

5.3.2 X-ray crystallographic study

Solid samples crystallize in orthorhombic $P2_12_12_1$, 2,2'-(((*S*)-1-phenylethyl)azanediyl)bis(*N*-((*S*)-1-phenylethyl)acetamide) *S,S,S*-**6**, 2,2'-((*R*)-1-phenylethyl)azanediyl)bis(*N*-((*R*)-1-phenylethyl)acetamide) *R,R,R*-**7**, 2,2'-(benzylazanediyl)bis(*N*-((*S*)-1-phenylethyl)acetamide) *S,S*-**10** and 2,2'(benzylazanediyl)bis(*N*-((*R*)-1-phenylethyl)acetamide) *R,R*-**11**, centrosymmetric space groups. The *ORTEP* view at 50 % probability for these compounds are shown in Figure 2. Details about data collection, refinement, and structure solution are recorded in (Table 4), and selected geometrical parameters are tabulated in Table 5. The structural parameters are found to be in the normal range. The experimentally obtained structural parameters are comparable with the similar parameters obtained theoretically by DFT level calculations.

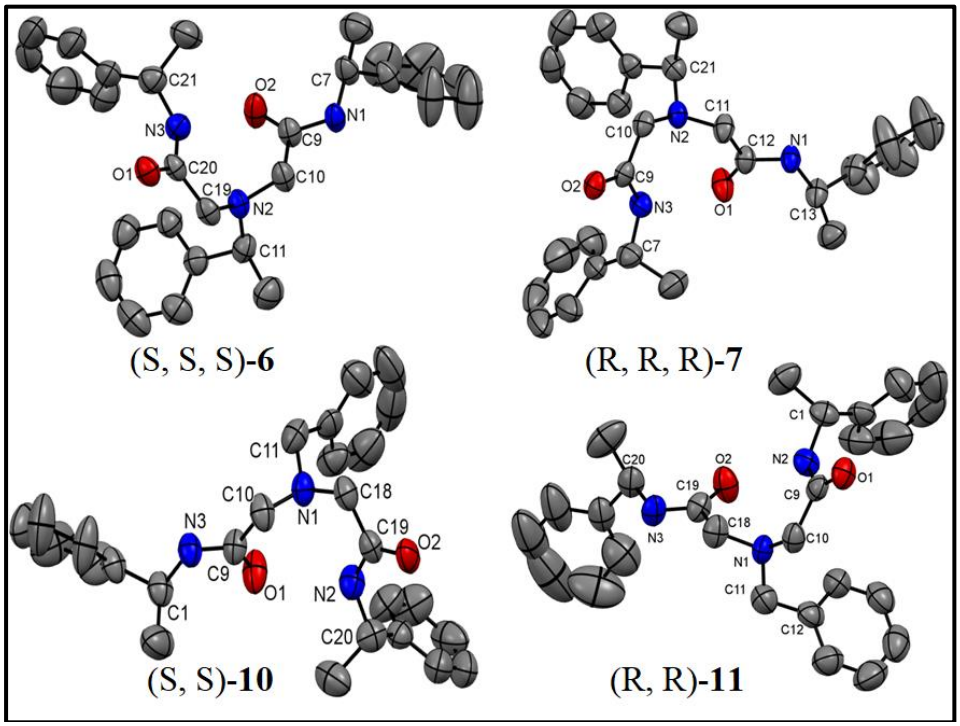

Figure 2. The ORTEP diagram with partial atom numbering showing 50 % probability ellipsoid; (hydrogen atoms are omitted for clarity).

Table 4. Crystal data and structure refinement for the compounds under investigation.

Identification code	*S,S,S*-**6**	*R,R,R*-**7**	*S,S*-**10**	*R,R*-**11**
Empirical formula	$C_{28}H_{33}N_3O_2$	$C_{28}H_{33}N_3O_2$	$C_{54}H_{62}N_6O_4$	$C_{54}H_{62}N_6O_4$
Formula weight	443.57	443.57	859.1	859.1
Temperature/K	293	293	293	293
Crystal system	orthorhombic	orthorhombic	orthorhombic	orthorhombic
Space group	$P2_12_12_1$	$P2_12_12_1$	$P2_12_12_1$	$P2_12_12_1$
a/Å	12.3633(7)	12.3650(8)	12.4639(12)	12.4959(15)
b/Å	13.2053(6)	13.1992(7)	13.0580(11)	13.0628(17)
c/Å	15.5757(8)	15.5514(8)	30.892(3)	30.927(4)
α/°	90	90	90	90
β/°	90	90	90	90
γ/°	90	90	90	90
Volume/Å^3	2542.9(2)	2538.1(2)	5027.9(8)	5048.2(11)
Z	4	4	4	4
ρ_{calc}g/cm^3	1.159	1.161	1.135	1.13
μ/mm^{-1}	0.073	0.074	0.072	0.072
F(000)	952	952	1840	1840
Radiation	MoKα (λ = 0.71073)	MoKα (λ = 0.71073)	MoKα (λ = 0.71073)	MoKα (λ = 0.71073)
2Θ range for data collection/°	6.92 to 58.54	6.6 to 58.1	6.12 to 58.2	6.12 to 46.8
Index ranges	$-16 \le h \le 15$, $-17 \le k \le 17$, $-19 \le l \le 20$	$-16 \le h \le 16$, $-16 \le k \le 15$, $-20 \le l \le 20$	$-16 \le h \le 16$, $-16 \le k \le 17$, $-41 \le l \le 40$	$-13 \le h \le 13$, $-14 \le k \le 14$, $-33 \le l \le 33$
Reflections collected	15453	15812	55456	20459
Independent reflections	5931 [R_{int} = 0.0638, R_{sigma} = 0.1020]	5943 [R_{int} = 0.0671, R_{sigma} = 0.1161]	12128 [R_{int} = 0.1251, R_{sigma} = 0.1349]	6469 [R_{int} = 0.0914, R_{sigma} = 0.1149]
Data/restraints/parameters	5931/10/301	5943/48/301	12128/6/581	6469/6/581
Goodness-of-fit on F^2	0.892	0.894	0.884	1.013
Final R indexes [I>=2σ (I)]	R_1 = 0.0657, wR_2 = 0.1460	R_1 = 0.0661, wR_2 = 0.1402	R_1 = 0.0735, wR_2 = 0.1642	R_1 = 0.0680, wR_2 = 0.0977
Final R indexes [all data]	R_1 = 0.1677, wR_2 = 0.2021	R_1 = 0.1729, wR_2 = 0.2000	R_1 = 0.2127, wR_2 = 0.2301	R_1 = 0.1513, wR_2 = 0.1277
Larg. diff. peak/hole /eÅ^{-3}	0.12/-0.14	0.15/-0.14	0.15/-0.15	0.15/-0.16

Table 5. Selected bond length and bond angles of Compound *S,S,S*-**6,** *R,R,R*-**7**, *S,S*-**10** and *R,R*-**11**.

Componds	Selected Bond	Bond Lengths(Å)	Selected Bond	Bond angles(º)
S,S,S-**6**	N3-C21	1.443(5)	O1-C20-N3	123.9(3)
	N3-C20	1.321(4)	O1-C20-C19	118.9(3)
	O1-C20	1.241(4)	O2-C9-C10	121.8(3)
	C19-C20	1.506(5)	O2-C9-N1	123.4(3)
	N2-C19	1.455(4)	C10-N2-C11	113.9(3)
	N2-C11	1.455(4)	C10-N2-C19	115.5(3)
	N2-C10	1.457(4)	C11-N2-C19	115.1(3)
	C9-C10	1.528(5)		
	O2-C9	1.227(4)		
	N1-C9	1.333(4)		
	N1-C7	1.466(4)		
R,R,R-**7**	N2-C21	1.461(4)	O1-C12-N1	123.7(3)
	N2-C11	1.460(4)	O1-C12-C11	121.7(3)
	C11-C12	1.529(5)	O2-C9-C10	119.1(3)
	O1-C12	1.225(4)	O2-C9-N3	123.3(3)
	N1-C12	1.336(4)	C10-N2-C11	115.4(3)
	N1-C13	1.466(5)	C10-N2-C21	115.2(3)
	N2-C10	1.453(4)	C11-N2-C21	114.3(3)
	C9-C10	1.502(5)		
	O2-C9	1.248(4)		
	N3-C9	1.319(4)		
	N3-C7	1.452(5)		
S,S-**10**	N1-C11	1.451(5)	O1-C9-N3	123.7(4)
	N1-C18	1.456(5)	O1-C9-C10	120.6(4)
	C18-C19	1.496(6)	O2-C19-C18	120.5(4)
	O2-C19	1.243(5)	O2-C19-N2	122.7(4)
	N2-C19	1.320(5)	C10-N1-C11	114.2(3)
	N2-C20	1.449(5)	C10-N1-C18	115.5(3)
	N1-C10	1.454(5)	C11-N1-C18	115.2(3)
	C9-C10	1.521(5)		
	O1-C9	1.231(4)		
	N3-C9	1.316(5)		
	C1-N3	1.474(5)		
R,R-**11**	N1-C11	1.446(6)	O1-C9-N2	124.4(5)
	C11-C12	1.509(7)	O1-C9-C10	120.2(6)
	N1-C10	1.460(7)	O2-C19-C18	121.5(5)
	C9-C10	1.526(7)	O2-C19-N3	122.4(5)
	O1-C9	1.232(6)	C10-N1-C11	116.3(5)
	N2-C9	1.344(7)	C10-N1-C18	115.4(5)
	N2-C1	1.457(6)	C11-N1-C18	112.2(5)
	N1-C18	1.459(6)		
	C18-C19	1.504(7)		
	O2-C19	1.242(6)		
	N3-C20	1.463(6)		

Table 6. Significant inter and intra molecular interaction interatomic distance (Å) found in compound *S,S,S*-**6,** *R,R,R*-**7**, *S,S*-**10** and *R,R*-**11**.

Componds	D-H---A	D-H	H---A	D---A
S,S,S-**6**	O1-H1---N1 (intermolecular)	2.087	0.860	2.939
	O2-H3---N3 (intramolecular)	2.122	0.860	2.932
R,R,R-**7**	O2-H3---N3 (intermolecular)	2.086	0.860	2.938
	O1-H2---N2 (intramolecular)	2.121	0.860	2.931
S,S-**10**	O1-H1---N1 (intermolecular)	2.067	0.861	2.900
	O2-H3---N3 (intramolecular)	2.152	0.859	2.986
R,R-**11**	O1-H3---N3 (intermolecular)	2.034	0.861	2.859
	O2-H3---N3 (intramolecular)	2.116	0.858	2.973

Notably, X-ray crystallography revealed the propensity of amidic and amine groups of newly synthesized amines to form intra- and intermolecular hydrogen bonding (Figure 3, Table 6). Interestingly molecule of *S,S,S*-**6** and *S,S*-**10** with similar intermolecular contacts vis. NH…O (~2.1 Å, intra-molecular) and donor-acceptor NH…O (~2.9 Å, intermolecular) H-bonding contacts lead to the formation of a fascinating 1D helical (P-type) supramolecular structure with helical pitch of ~12.3 Å (Figure 4a). While molecules of R, R, R-**10** and R, R-**11** with similar intermolecular contacts vis. NH…O (~2.1 Å, intra-molecular) and donor-acceptor NH…O (~2.9 Å, intermolecular) H-bonding contacts lead to the formation of opposite 1D helical (M-type) supramolecular structure with helical pitch of ~12.3 Å (Figure 4b).

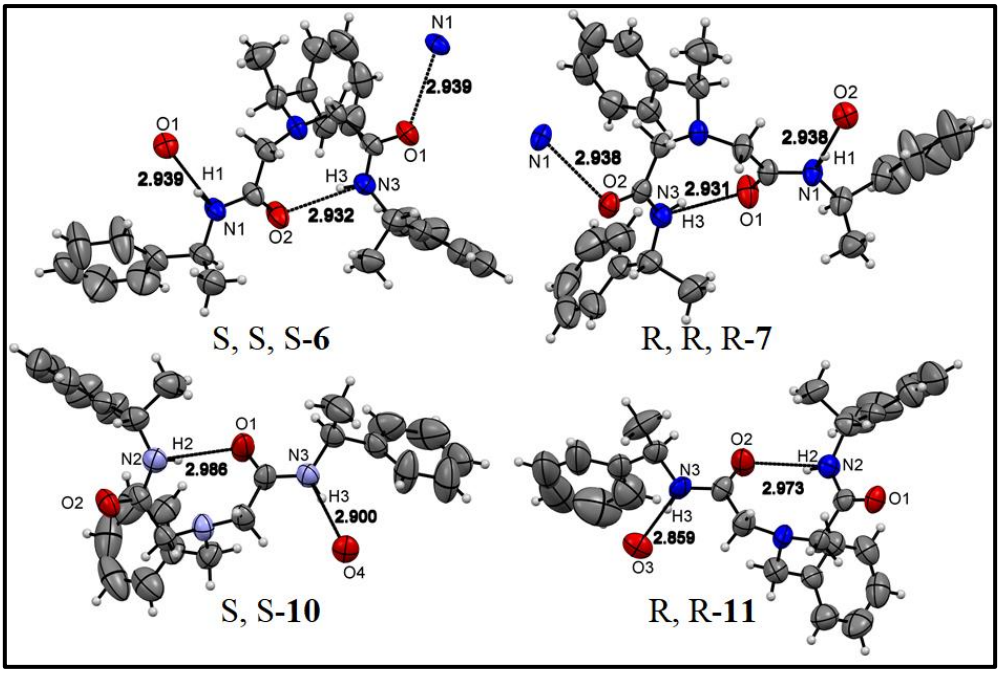

Figure 3. Crystallographic study reveals the propensity of synthesized ligand to form inter and intramolecular H-bonding.

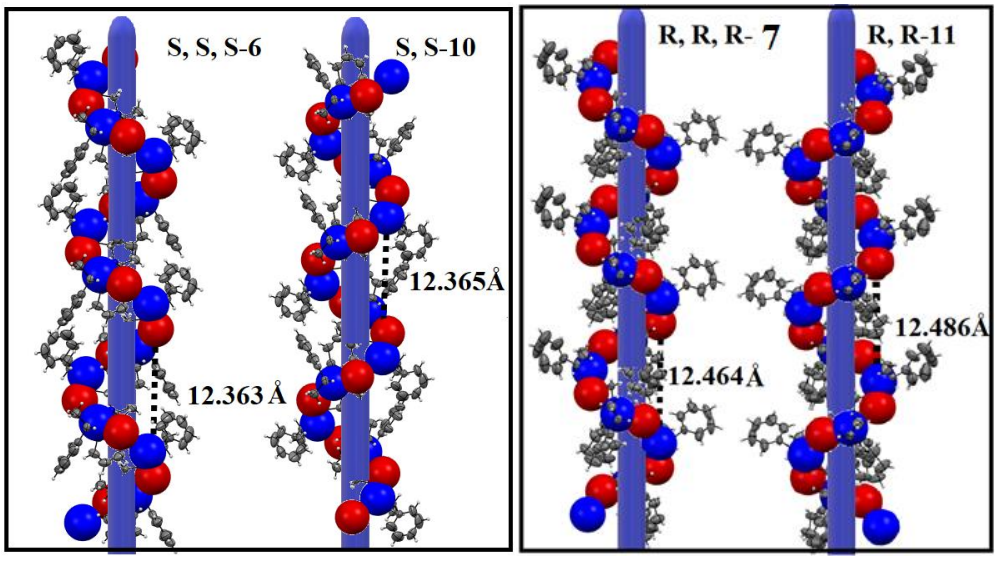

(a) **(b)**

Figure 4. (a) Molecule of *S,S,S*-**6** and *S,S*-**10** forming fascinating 1D P-helix through NH-O (inter) and NH-O (intra) with helical pitch of ~12.3 Å. (b) Molecule of *R,R,R*-**7** and *R,R*-**11** forming fascinating 1D M-helix through NH-O (inter) and NH-O (intra) with helical pitch of ~12.3 Å.

The presence of chirality at the amidic N-substituent is found to be crucial for formation of diverse helical motifs. For example, The S, S-chirality leads to the formation of M-helix whereas R, R-chirality leads to the formation of P-type of helical arrangement.

5.3.3 Theoretical Investigations.

5.3.3.1 Density functional theory calculations

All the calculations were carried out using the Gaussian 16 program suite and molecular orbitals were generated by GaussView 6.0 program.[17] Full geometry optimizations of (S, S)-**1**, (R, S)-**2**, (R, R)-**3**, (S, R)-**4, 5**, (S, S, S)-**6**, (R, R, R)-**7**, (S, S, R)-**8**, (R, R, S)-**9**, (S, S)-**10**, (R, R)-**11**, (S,)-**12** and (R)-**13** were performed using density functional theory (DFT) at B3LYP basis sets. These calculations were used to analyses frontier molecular orbitals, HOMO–LUMO energy gap and mapping of electrostatic potential surface to get insights of structural details. An optimized geometry for the minimum energy conformation for *S,S*-**1,** *R,S*-**2,** *R,R*-**3,** S,*R*-**4; 5,** *S,S,S*-**6,** *R,R,R*-**7,** *S,S,R*-**8,** *R,R,S*-**9,** *S,S*-**10,** *R,R*-**11,** *S*-**12** and *R*-**13** are shown in Figure. 5. The HOMO-LUMO gaps (Figure 6) and the energy of optimized geometry for all the compounds have been summarized in Table 7.

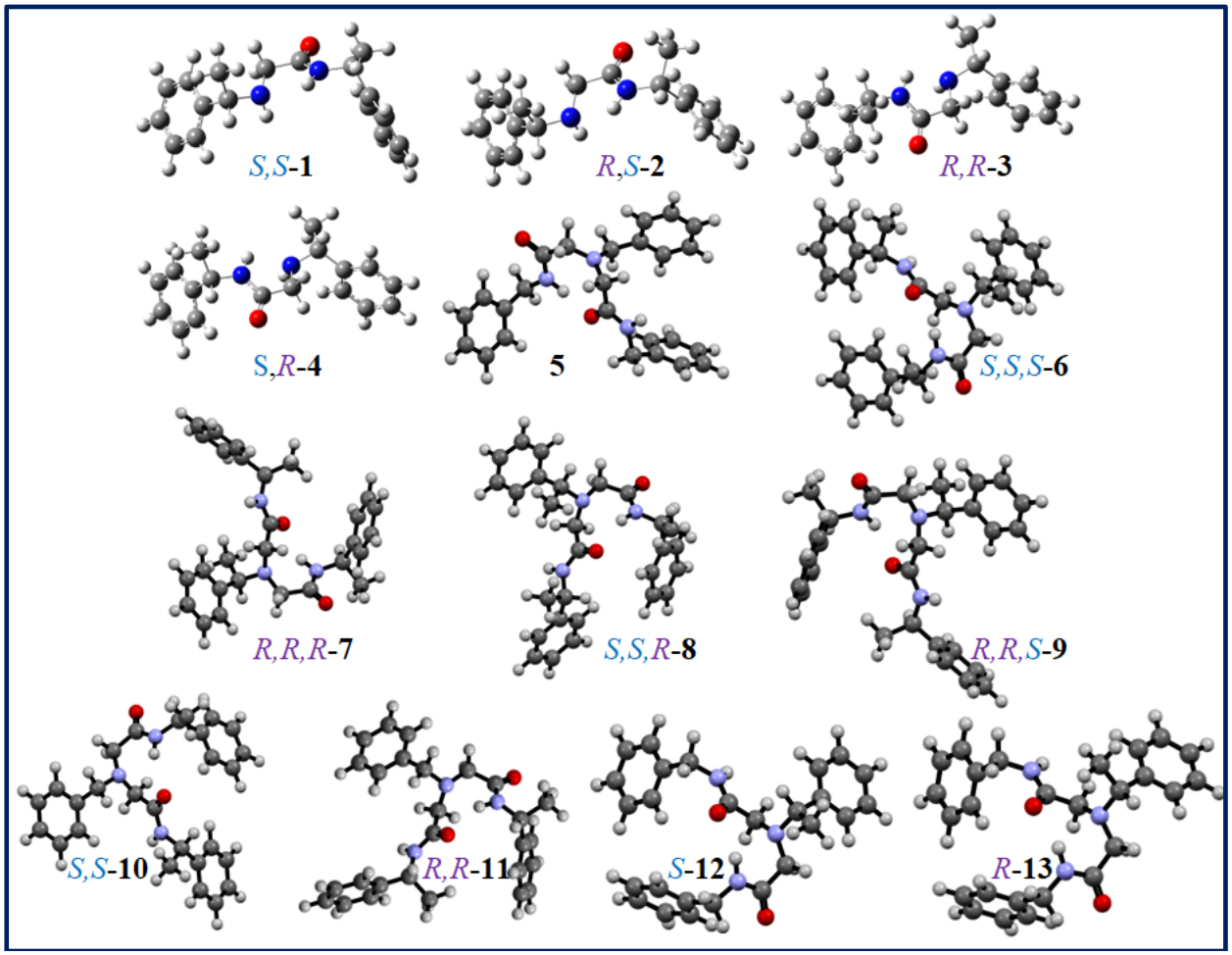

Figure 5. An optimized geometry for the minimum energy conformation of compounds *S,S*-**1,** *R,S*-**2,** *R,R*-**3**, S,*R*-**4; 5,** *S,S,S*-**6,** *R,R,R*-**7,** *S,S,R*-**8,** *R,R,S*-**9,** *S,S*-**10,** *R,R*-**11,** *S*-**12** and *R*-**13**
at B3LYP/LanL2DZ level.

Table 7. Summary of DFT study performed on B3LYP/6-31G(d,P) levels

Entry	Energy of Optimized Geometry (Hartree)	Dipole moment (Debye)	$E_{HOMO-LUMO}$ (eV)	$E_{HOMO-LUMO}$ (eV)	λ_{max} cal. (exp) nm
S,S-**1**	-883.942	3.59	-6.1759, -0.1853	5.990	206 (255)
R,S-**2**	-883.946	3.64	-6.2303, -0.2147	6.015	206 (259)
R,R-**3**	-883.943	3.70	-6.2232, -0.2299	5.993	206 (256)
S,*R*-**4**	-883.940	3.62	-6.1916, -0.2111	5.980	207 (267)
5	-1283.32	7.92	-5.4162, -0.5363	4.880	254 (252)
S,S,S-**6**	-1401.64	5.73	-5.7558, -0.4084	5.347	231 (252)
R,R,R-**7**	-1401.64	6.16	-5.7661, -0.4512	5.315	231 (253)
S,S,R-**8**	-1401.64	5.80	-5.7919, -0.4101	5.382	233 (252)
R,R,S-**9**	-1401.64	6.15	-5.7051, -0.4574	5.248	230 (252)
S,S-**10**	-1362.33	5.76	-5.7949, -0.4174	5.378	230 (252)
R,R-**11**	-1362.32	6.23	-5.7402, -0.4705	5.270	235 (252)
S-**12**	-1323.01	5.37	-5.7721, -0.3045	5.408	229 (253)
R-**13**	-1323.01	5.44	-5.8270, -0.3075	5.520	224 (252)

The UV-visible λ_{max} values determined experimentally matches well with the calculated values (Table 7) and this validate the optimized structures for all the compounds under investigation. Moreover, HOMO-LUMO energy gaps obtained (Figure 6) for *S,S*-**1,** *R,S*-**2,** *R,R*-**3,** S,*R*-**4**, **5,** *S,S,S*-**6,** *R,R,R*-**7,** *S,S,R*-**8,** *R,R,S*-**9,** *S,S*-**10,** *R,R*-**11,** *S*-**12** and *R*-**13** falls in the range of 4.8-6.0 eV and this suggests non-conducting nature of the compounds.

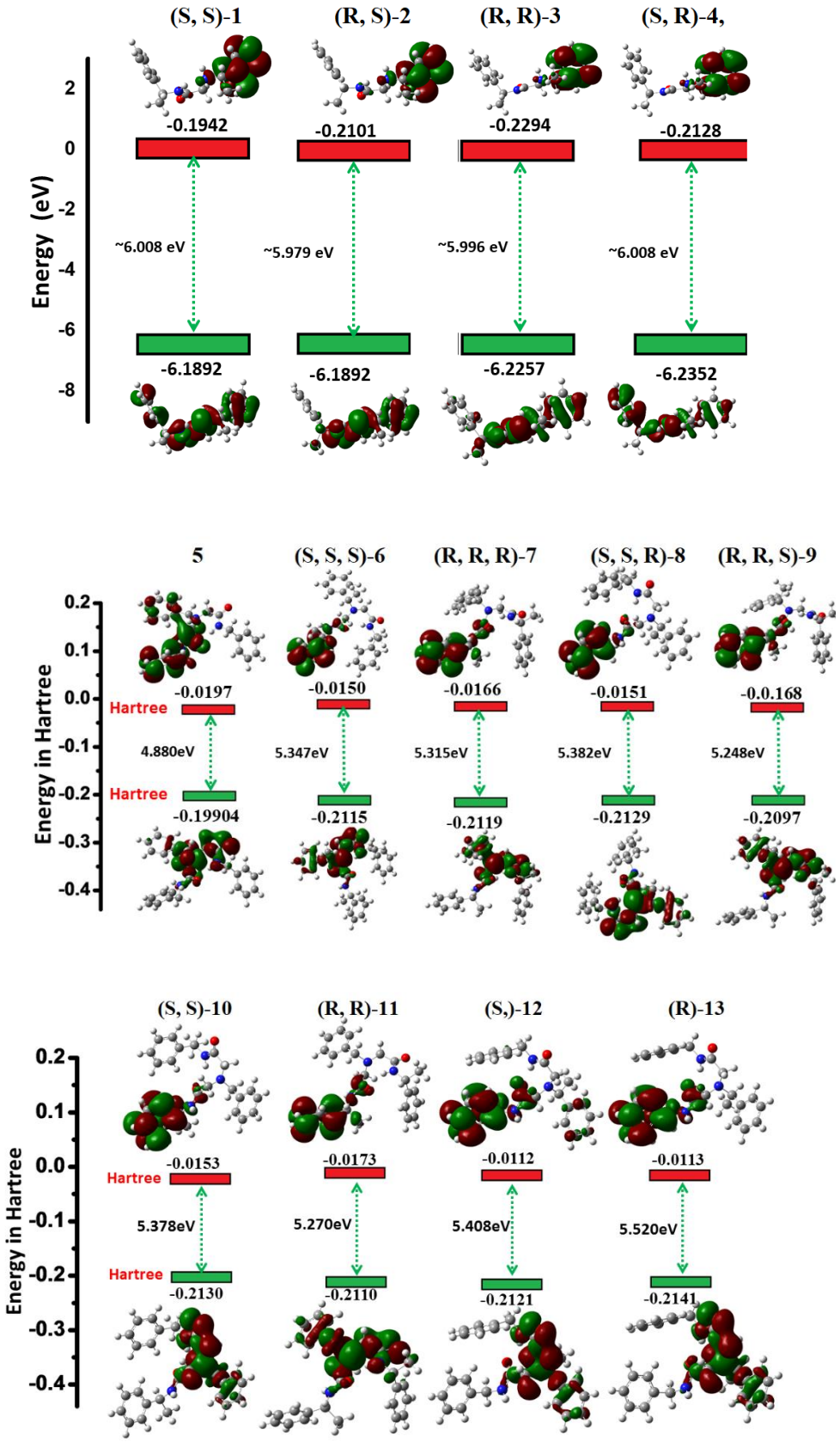

Figure 6. Determination of HOMO-LUMO gaps for *S,S*-**1,** *R,S*-**2,** *R,R*-**3,** *S,R*-**4; 5,** *S,S,S*-**6,** *R,R,R*-**7,** *S,S,R*-**8,** *R,R,S*-**9,** *S,S*-**10,** *R,R*-**11,** *S*-**12** and *R*-**13** in eV.

5.3.3.2 Molecular electrostatic potential

The molecular electrostatic potential (MESP) of chemical species plays a decisive factor for determining the properties and potential sites associated to the reactivity in biological systems and processes. In the mapping of electrostatic potential surface (Figure. 7), the occurrence of negative potential over the amide oxygen and positive potential is around the amide proton are mainly responsible for the existence of donor-acceptor intermolecular contacts involving amidic groups in the molecules which is well supported by crystallographic study.

S,*S*-**1**

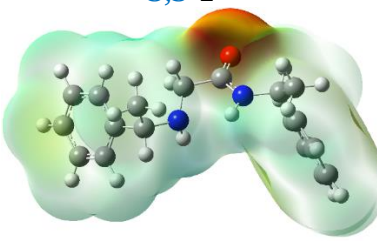

R,*S*-**2**

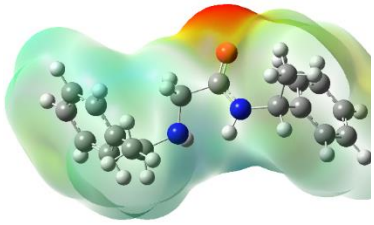

R,*R*-**3**

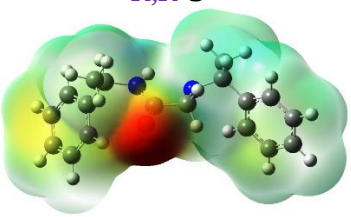

S,*R*-**4**

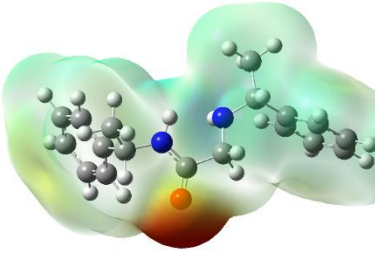

5

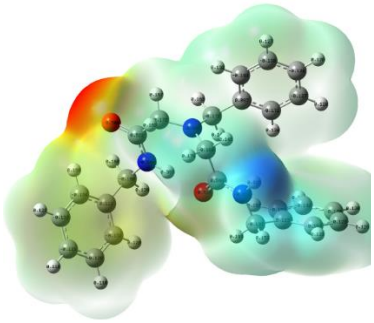

S,*S*,*S*-**6**

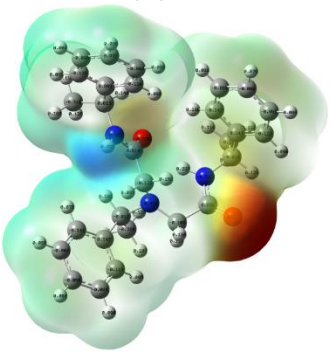

R,*R*,*R*-**7**

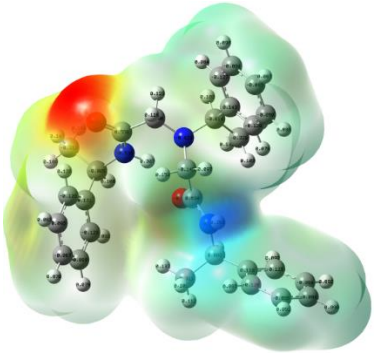

S,*S*,*R*-**8**

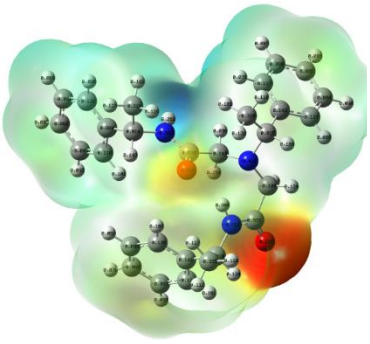

R,*R*,*S*-**9**

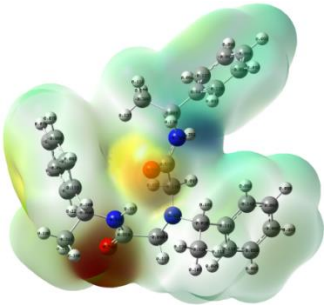

S,*S*-**10**

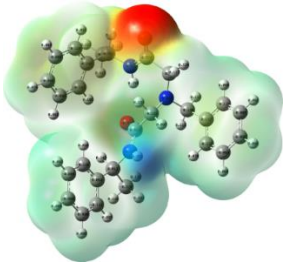

R,*R*-**11**

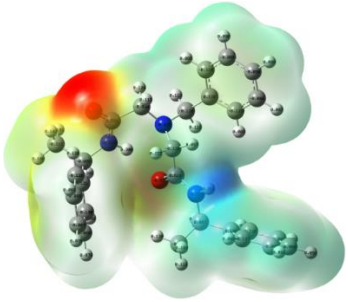

S-**12**

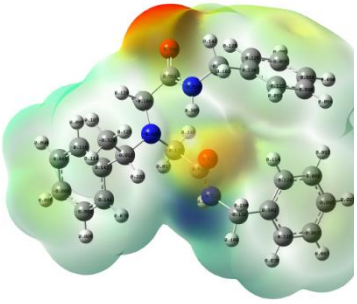

R-**13**

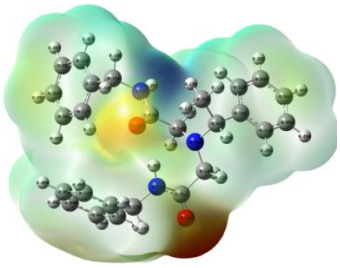

Figure 7. Representations of electron density from total SCF density (Isovalue= 0.0004; mapped with ESP).

Preliminary investigation of the tertiary amine compounds **5-13** holding a greater number of biologically relevant groups for their cytotoxicity against MDA-MB-231 carcinoma cell line by MTT assay have been caried out and the results are summarized in Figure 8. All the compounds showed cytotoxic activity against in low micro-molar concentrations. However, we are in the studying all the molecules for their potential biological applications in detail by using various other cell lines.

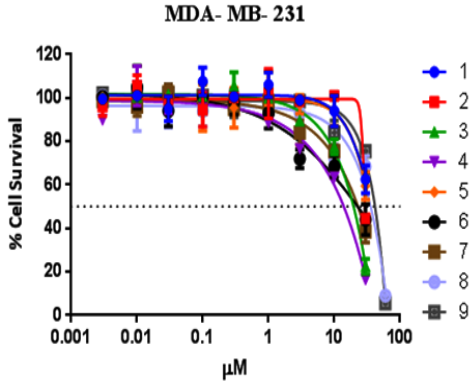

Compounds	IC50 values (µM) MDA-MB-231
5	38.3
S,S,S-**6**	29.2
R,R,R-**7**	19.7
S,S,R-**8**	14.8
R,R,S-**9**	34.8
S,S-**10**	22.4
R,R-**11**	22.3
S-**12**	35.4
R-**13**	41.5

(a) **(b)**

Figure 8. (a) Cytotoxicity of compounds 5-13 against MDA-MB-231 carcinoma cell line. (b) In vitro cytotoxicity on MDA-MB-231cell line after 24 hours of exposure of 5-13.

5.4 Conclusion

In summary, synthesis and characterization of several organic chiral secondary amines viz. *S,S*-**1**, *R,S*-**2**, *R,R*-**3** and *S,R*- **4** and **5,** *S,S,S*-**6,** *R,R,R*-**7,** *S,S,R*-**8,** *R,R,S*-**9,** *S,S*-**10,** *R,R*-**11,** *S*-**12** and *R*-**13** have been accomplished. Further, a DFT level calculations have been performed to reinforce the experimental data. The single crystal X-ray diffraction (SCXRD) study confirms the ability of the molecules of *S,S,S*-**6,** *R,R,R*-**7,** *S,S*-**10** and *R,R*-**11** to form intra- and intermolecular NH…O hydrogen bonding interactions, which is supported by the mapping of electrostatic potentials of these molecules. The chirality related influence on the supramolecular

packing of the molecules has been observed. For instance, molecules holding *S*-chirality viz. *S,S,S*-**6** and *S,S*-**10** form a fascinating 1D helical (P-type) supramolecular structure while the molecules holding *R*-chirality viz. *R,R,R*-**10** and *R,R*-**11** form opposite 1D helical (M-type) supramolecular structure holding almost similar helical pitch of ~12.3 Å. All the compounds studied herein are non-conducting in nature as their band gap calculated at DFT level falls in the range of 4.8-6.0 eV. We have successfully utilized the chiral secondary amines viz. *S,S*-**1**, *R,S*-**2**, *R,R*-**3** and *S,R*- **4** to derivatise into their corresponding dithiocarbamate ligands and transition metal complexes and the outcomes of this is presented in the next chapter 6. We are in the process of screening all the molecules for their potential biological applications with the anticipation that some of the compounds would pronounce activity in the living system due the ability of the molecules to offer an effective hydrogen bonding interaction.

5.5 Reference

1. The Impact of Stereochemistry on Drug Development and Use, ed. H. Y. Aboul-Enein and I. W. Wainer, Wiley, New York, **1997**.
2. (a) E. L. Izake, *J. Pharm. Sci*., **2007**, 96, 1659; (b) J. H. Kim, A. R. Scialli, *Toxicol. Sci.*, **2011**,122,1.
3. (a) F. Arnesano, A. Pannunzio, M. Coluccio, G. Natile, *Coord. Chem. Rev.*, **2015**, 284, 286; (b) J. F. Vollano, S. Al-Baker J. C. Dabrowiak, J. E. Schurig, *J. Med. Chem.*, **1987**, 30, 716.
4. D. L. Ma, M. Wang, C. Liu, X. Miao, T. S. Kang, C. H. Leung, *Coord. Chem. Rev*. **2016**, 324, 90.
5. B. Kater, A. Hunold, H. G. Schmalz, L. Kater, B. Bonitzki, P. Jesse, A. Prokop, J. Cancer Res. Clin. Oncol. 2011, 137, 639.
6. C. J. Savani, D. R.Vennapu, H. Roy, V. K. Singh, *J. Organomet. Chem.* **2021**, 950, 121983.
7. C. J. Savani, H. Roy, S. K. Verma, D. R. Vennapu, V. K. Singh, *Appl. Organomet. Chem*. **2021**, 35, e6137.
8. (a) S. Bertelsen, A. Karl, *J. Chem. Soc. Rev*., **2009**, 38, 2178; (b) J. Seayad, B. List, *Org. Biomol. Chem*., **2005**, 3, 719.
9. M. Kumar, R. I. Kureshy, S. Saravanan, S. Verma, A. Jakhar, N.l H. Khan, S. H. R. Abdi, H. C. Bajaj, *Org. Lett*. **2014**, 16, 2798.

10. D. Wu, P. Cai, X. Zhao, Y. Pan, *Org. Lett*. **2017**, 19, 5018; (b) D. Ghislieri, N. Turner, *J. Top. Catal*. **2014**, 57, 284;(c) C. E. Paul, M. Rodríguez-Mata, E. Busto, I. Lavandera, V. Gotor-Fernández, V. Gotor, S. García-Cerrada, J. Mendiola, Ó. de Frutos, I. Collado, *Org. Process Res. Dev*. **2014**, 18, 788.
11. (a) M. Breuer, K. Ditrich, T. Habicher, B. Hauer, M. Kesseler, R. Stürmer, T. Zelinski, *Angew. Chem., Int. Ed*. **2004**, 43, 788; (b) A. Gomm, E. O'Reilly, *Curr. Opin. Chem. Biol*. **2018**, 43, 106.
12. (a) V. K. Singh, V. Pillai, S. K. Patel, L. Buch, *ChemistrySelect*, **2019**, 4, 8689; (b) V. Pillai, S. K. Patel, L. Buch, V. K. Singh, *Appl. Organometal Chem*., **2018**, 32, e4559.
13. (a) T. F. Wood and J. H. Gardner, *J. Am. Chem. Soc*. **1941**, 63, 2741; (b) N. C. Kapa, G. G. Muccioli, G. Labar, J. H. Poupaert and D. M. Lambert, *J. Med. Chem*. **2009**, 52, 7310. (c) W. Huang, Y. Ding, Y. Miao, M. -Z. Liu, Y. Li and G. -F. Yang, *Eur. J. Med. Chem*. **2009**, 44, 3687.
14. CrysAlispro program (Version 1.171.37.33) Agilent Technologies, **2014**.
15. G. M. Sheldrick, Acta Cryst., **2015**, C71, 3.
16. (a) O. V. Dolomanov, L. J. Bourhis, R. J. Gildea, J. A. K. Howard, H. Puschmann, *J. Appl. Cryst.*, **2009**, 42, 339; (b) L. J. Bourhis, O. V. Dolomanov, R. J. Gildea, J. A. K. Howard, H. Puschmann, *Acta Cryst*., **2015**, A71, 59.
17. M. J. Frisch, G. W. Trucks, H. B. Schlegel, G. E. Scuseria, M. A. Robb, J. R. Cheeseman, G. Scalmani, V. Barone, G. A. Petersson, H. Nakatsuji, X. Li, M. Caricato, A. V. Marenich, J. Bloino, B. G. Janesko, R. Gomperts, B. Mennucci, H. P. Hratchian, J. V. Ortiz, A. F. Izmaylov, J. L. Sonnenberg, D. Williams-Young, F. Ding, F. Lipparini, F. Egidi, J. Goings, B. Peng, A. Petrone, T. Henderson, D. Ranasinghe, V. G. Zakrzewski, J. Gao, N. Rega, G. Zheng, W. Liang, M. Hada, M. Ehara, K. Toyota, R. Fukuda, J. Hasegawa, M. Ishida, T. Nakajima, Y. Honda, O. Kitao, H. Nakai, T. Vreven, K. Throssell, J. A. Montgomery, Jr, J. E. Peralta, F. Ogliaro, M. J. Bearpark, J. J. Heyd, E. N. Brothers, K. N. Kudin, V. N. Staroverov, T. A. Keith, R. Kobayashi, J. Normand, K. Raghavachari, A. P. Rendell, J. C. Burant, S. S. Iyengar, J. Tomasi, M. Cossi, J. M. Millam, M. Klene, C. Adamo, R. Cammi, J. W. Ochterski, R. L. Martin, K. Morokuma, O. Farkas, J. B. Foresman, D. J. Fox, Gaussian, Inc. Wallingford CT, **2016**.

5.6 Annexures

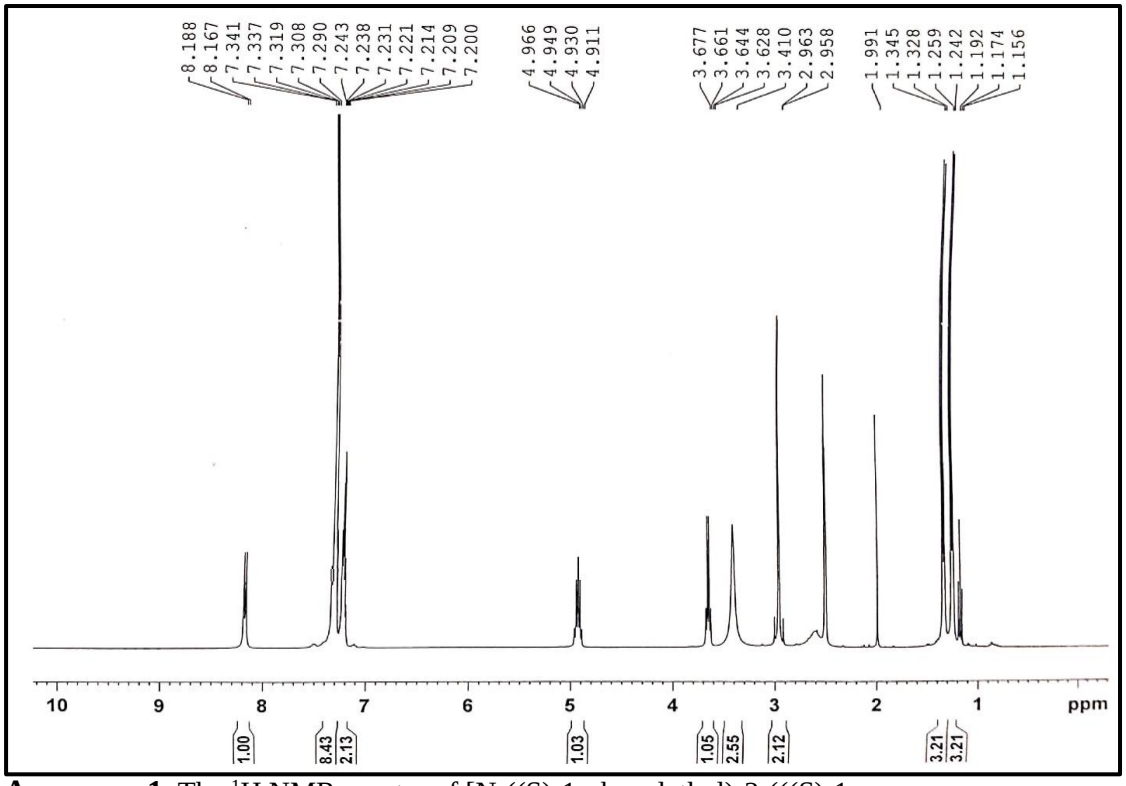

Annexure 1. The ^{1}H NMR spectra of [N-((S)-1-phenylethyl)-2-(((S)-1-henylethyl)amino)acetamide] *S*,*S*-**1.**

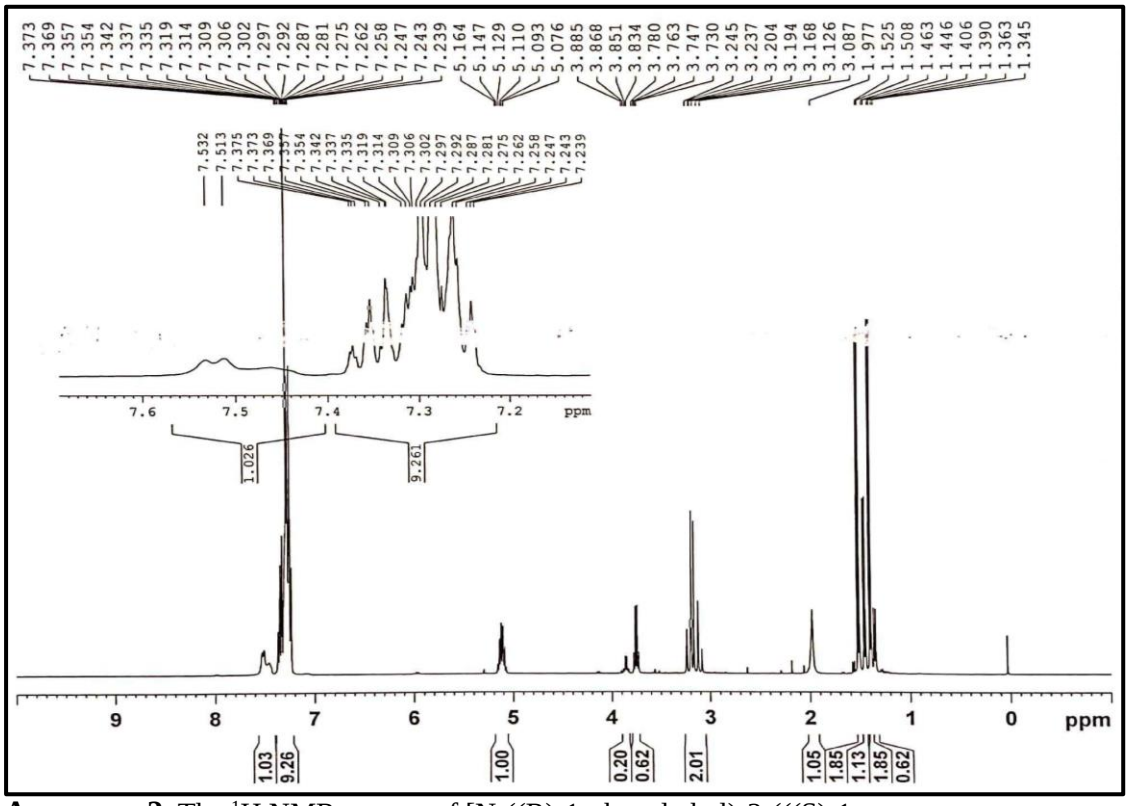

Annexure 2. The ^{1}H NMR spectra of [N-((R)-1-phenylethyl)-2-(((S)-1-henylethyl)amino)acetamide] *R*,*S*-**2.**

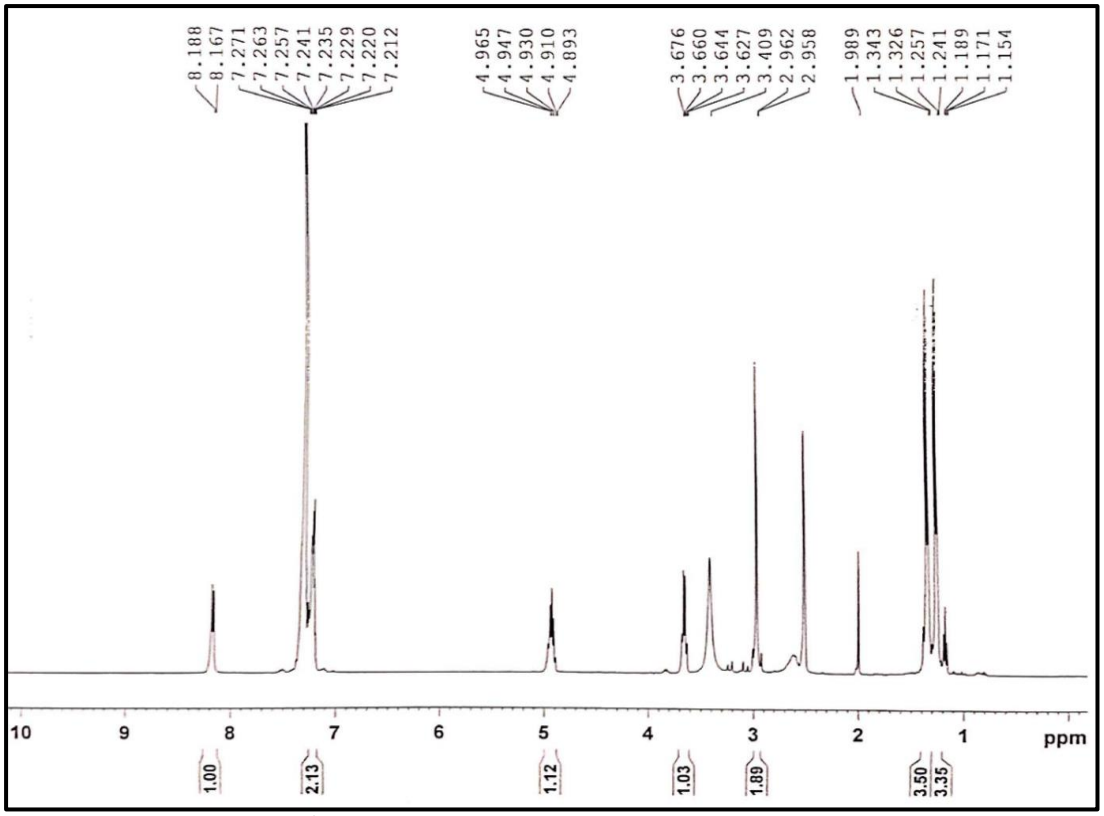

Annexure 3. The ^{1}H NMR spectra of [N-((R)-1-phenylethyl) -2-(((R)-1-phenylethyl)amino) acetamide] *R*,*R*-**3**.

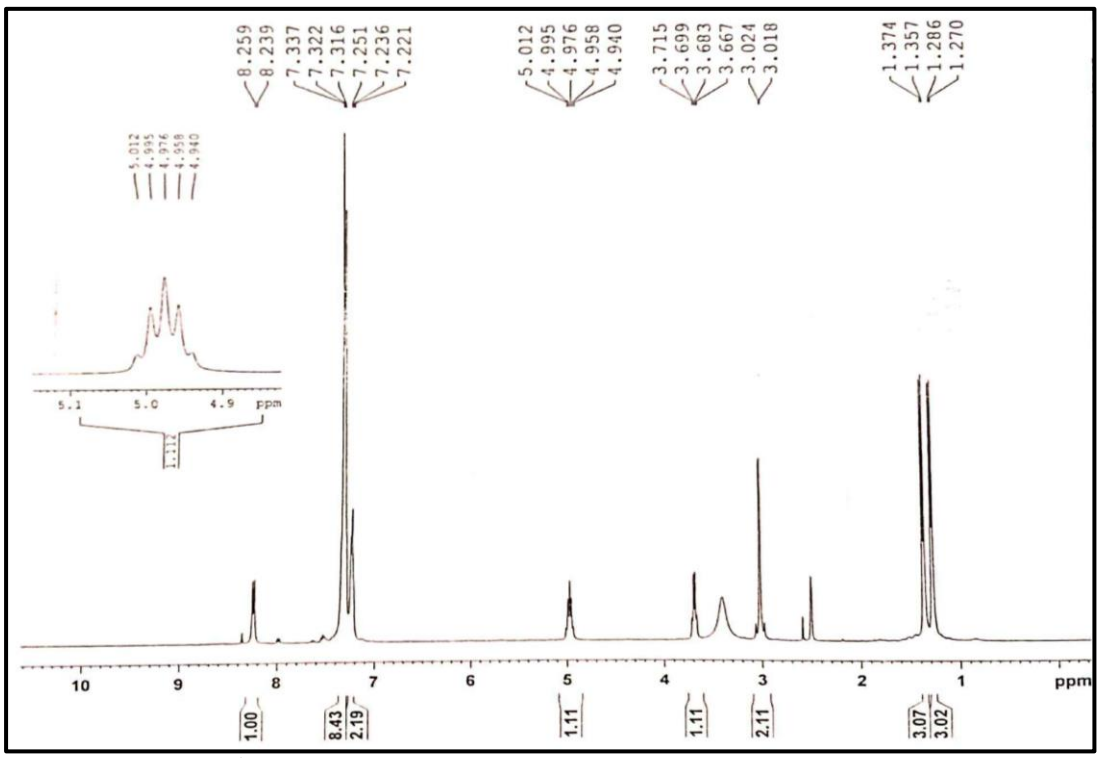

Annexure 4. The ^{1}H NMR spectra of [N-((S)-1-phenylethyl)-2-(((R)-1-phenylethyl)amino) acetamide] *S*,*R*-**4**.

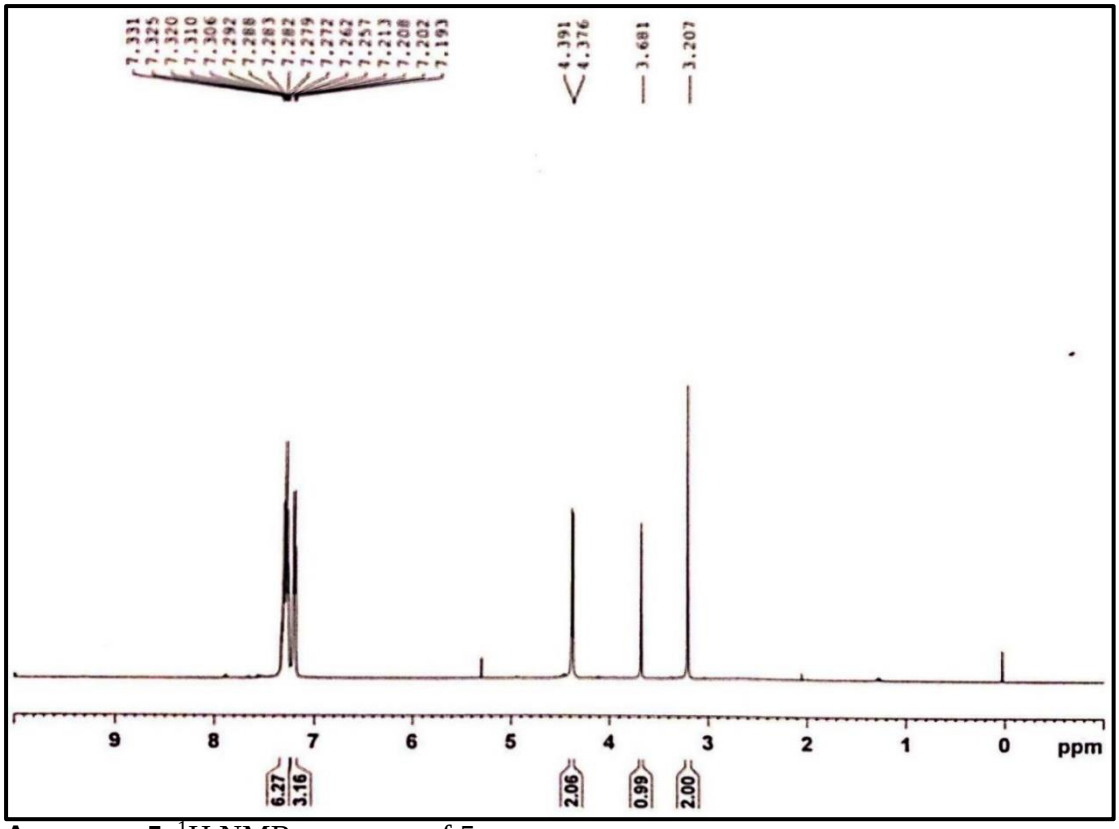

Annexure 5. ^{1}H NMR spectrum of 5.

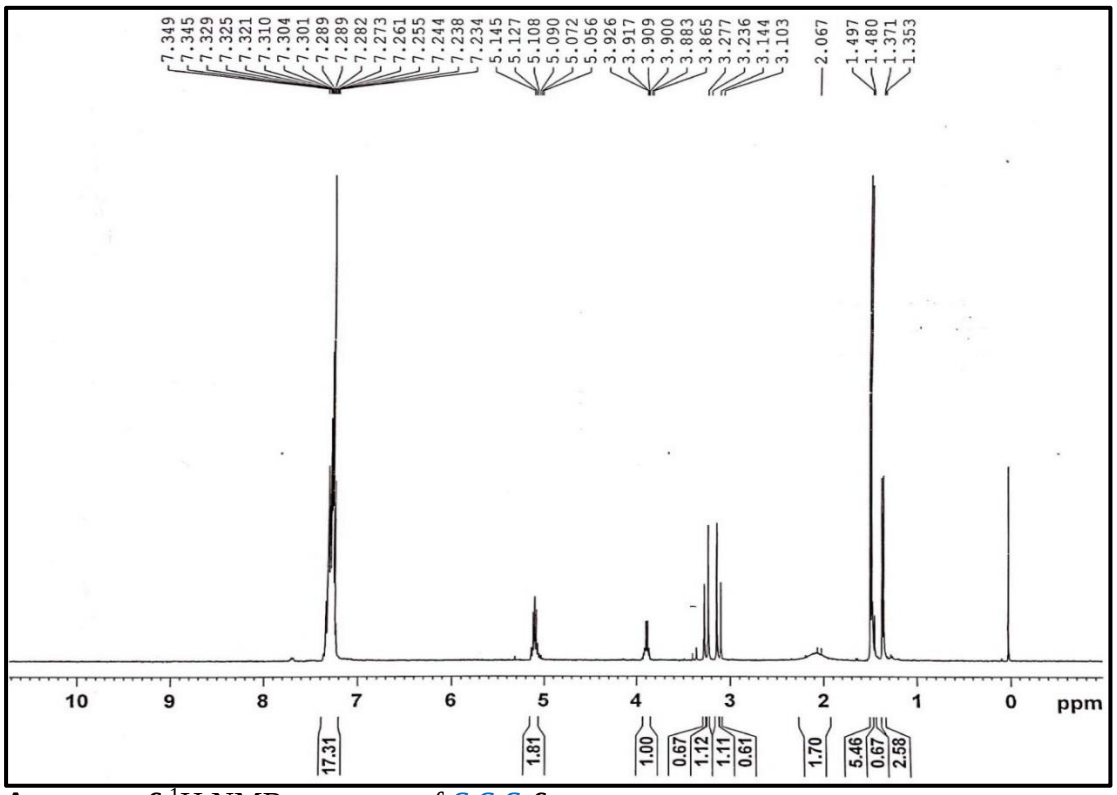

Annexure 6.^{1}H NMR spectrum of ***S,S,S*-6**.

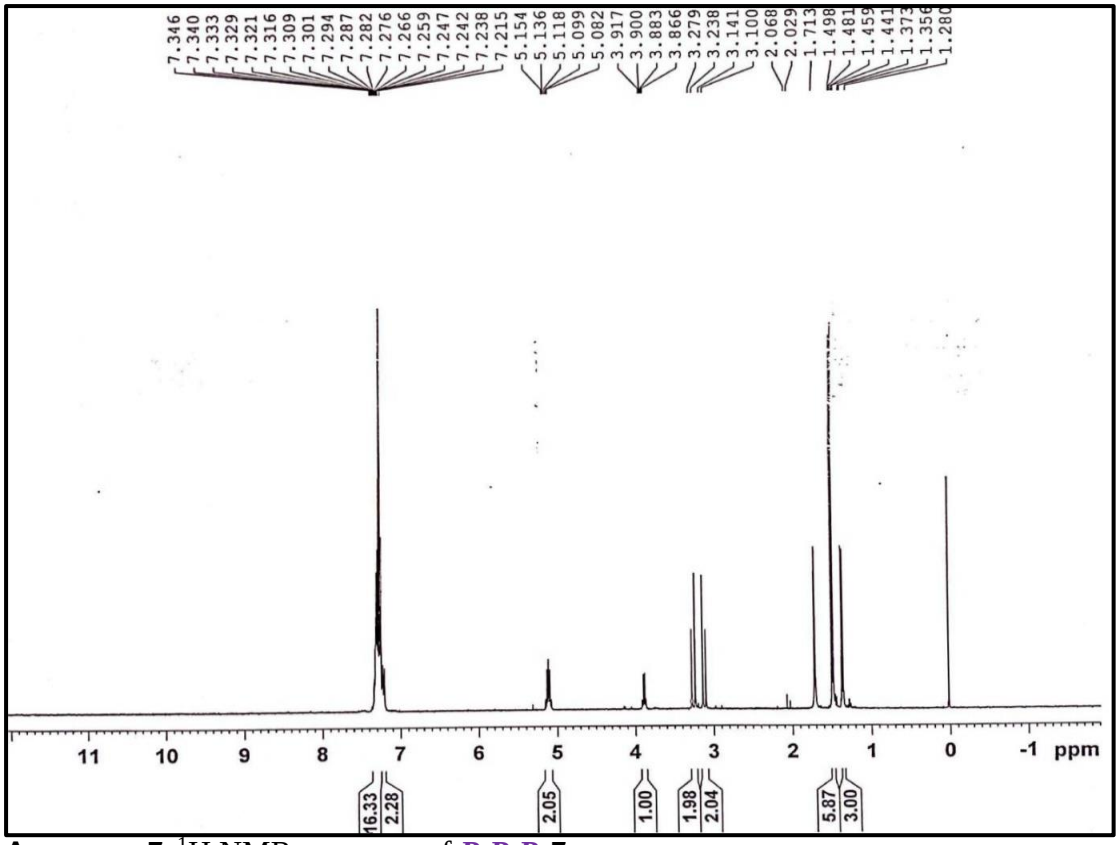

Annexure 7. ^{1}H NMR spectrum of ***R,R,R*-7**.

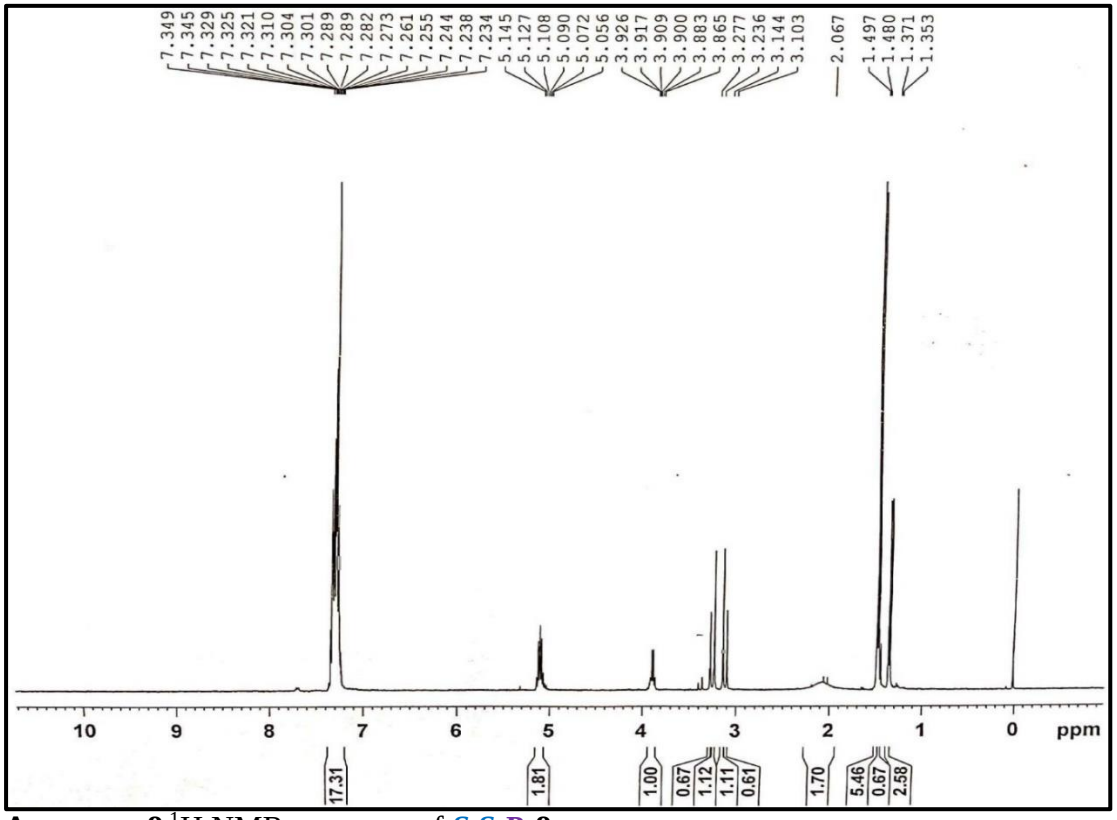

Annexure 8.^{1}H NMR spectrum of ***S,S,R*-8**.

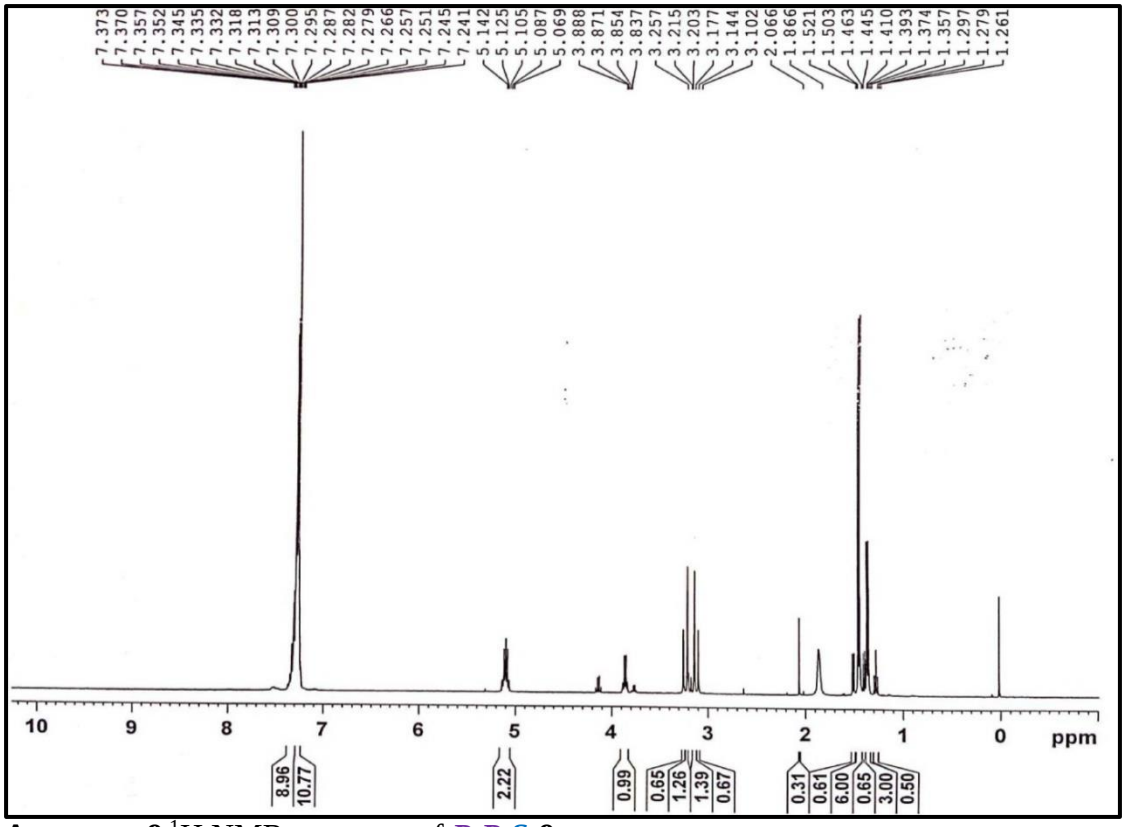

Annexure 9.[1]H NMR spectrum of ***R,R,S*-9**.

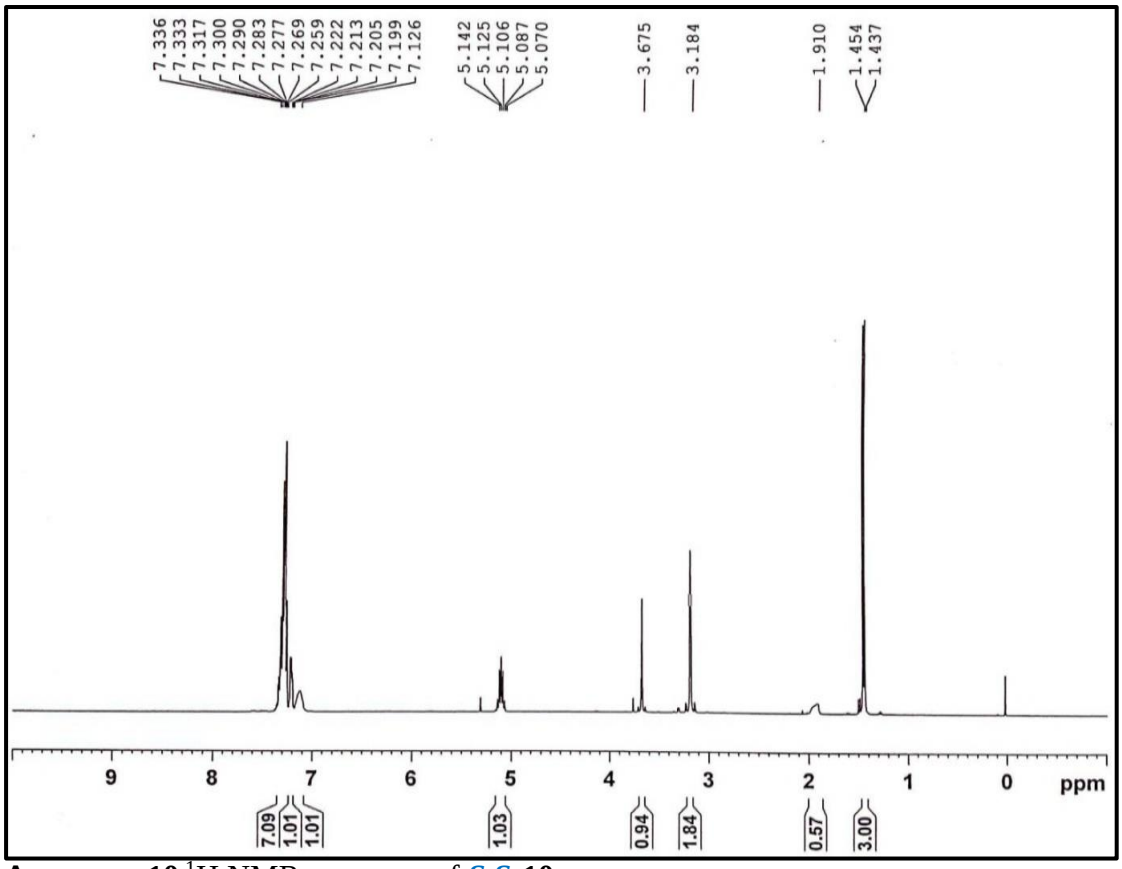

Annexure 10.[1]H NMR spectrum of ***S,S*-10**.

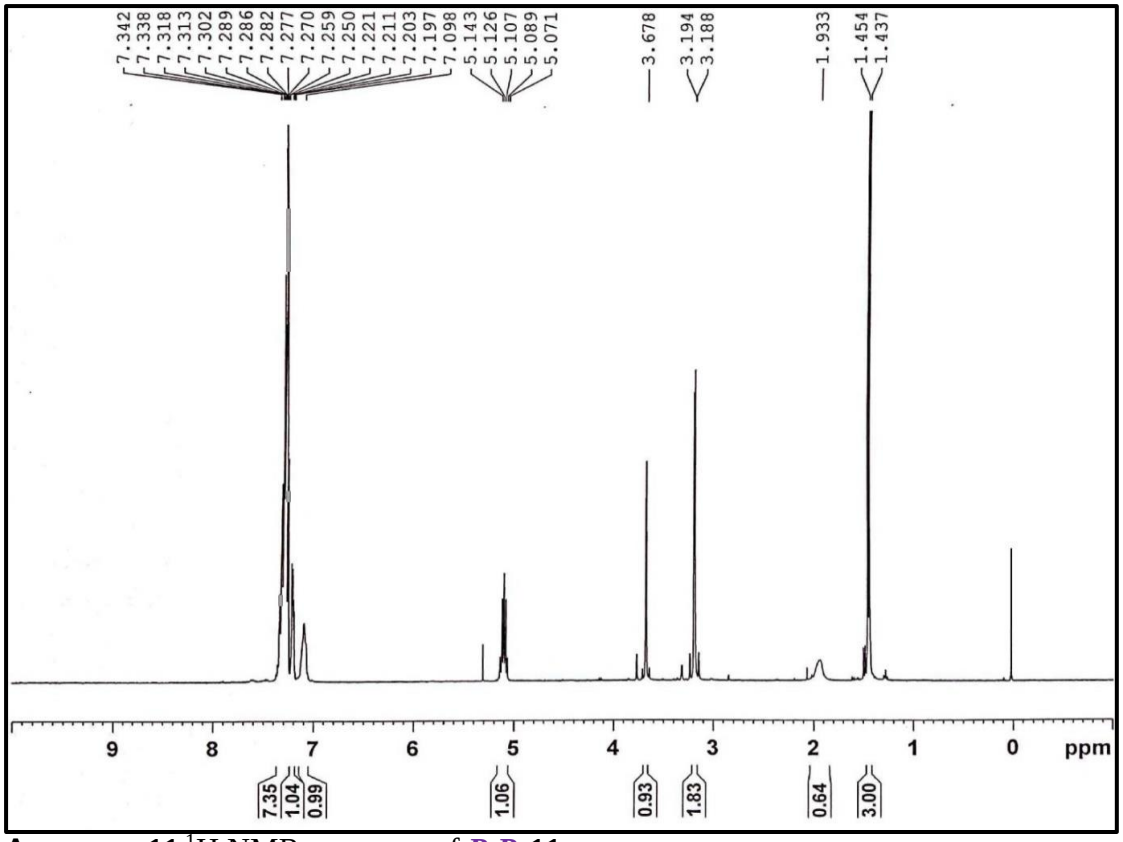

Annexure 11.[1]H NMR spectrum of ***R,R*-11**.

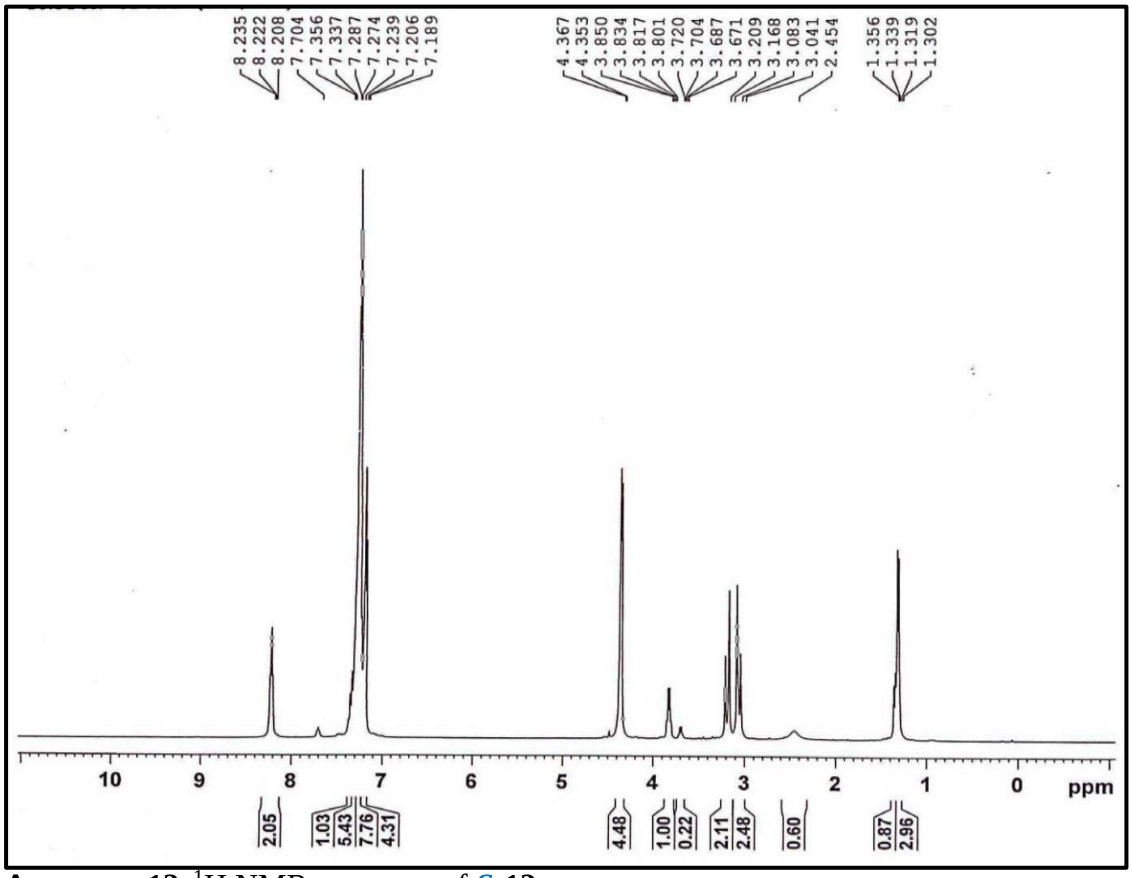

Annexure 12. [1]H NMR spectrum of ***S*-12**.

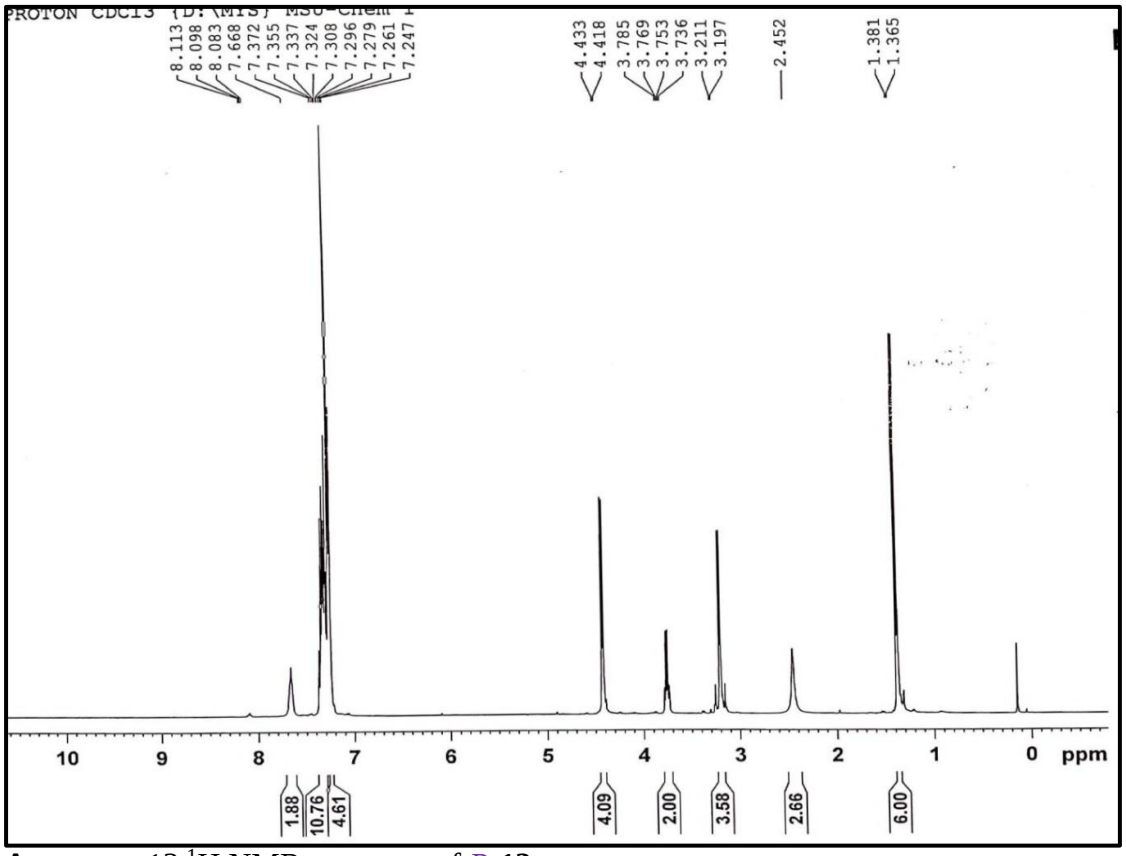

Annexure 13.[1]H NMR spectrum of *R*-**13**.

.

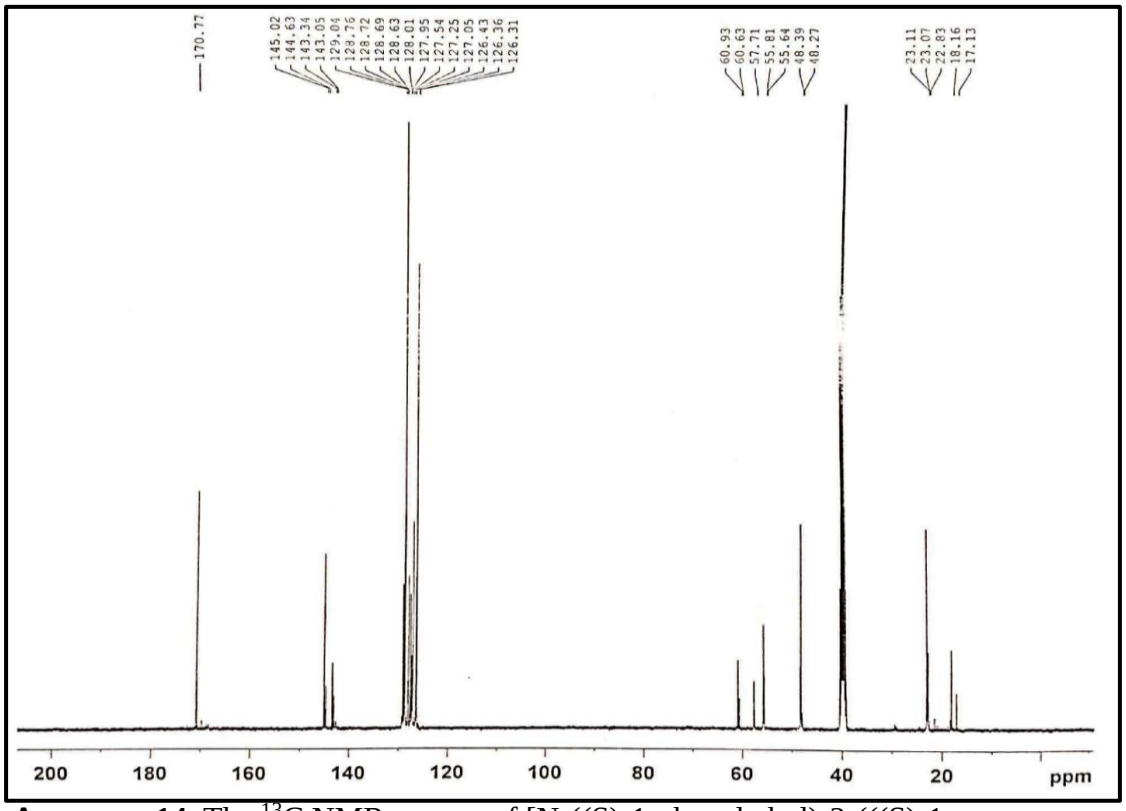

Annexure 14. The [13]C NMR spectra of [N-((S)-1-phenylethyl)-2-(((S)-1-phenylethyl)amino) acetamide] ***S,S*-1**.

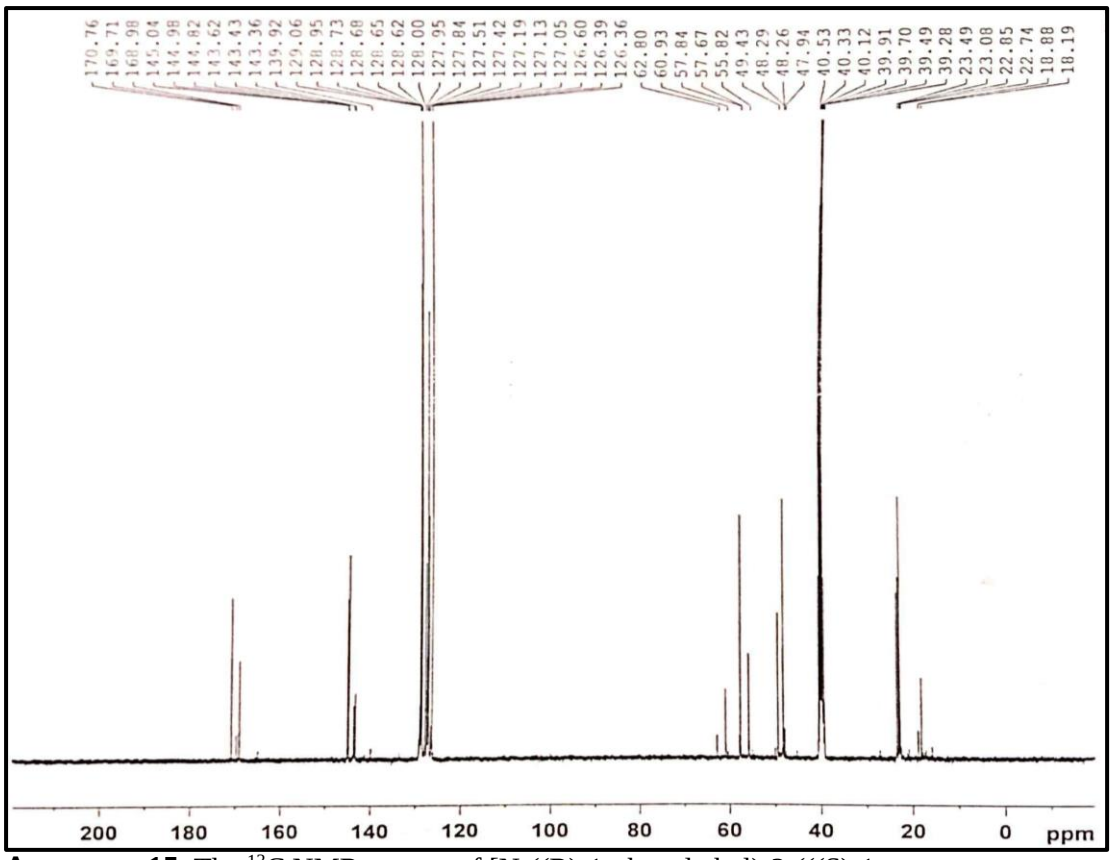

Annexure 15. The ^{13}C NMR spectra of [N-((R)-1-phenylethyl)-2-(((S)-1-phenylethyl)amino) acetamide] *R*,*S*-**2**.

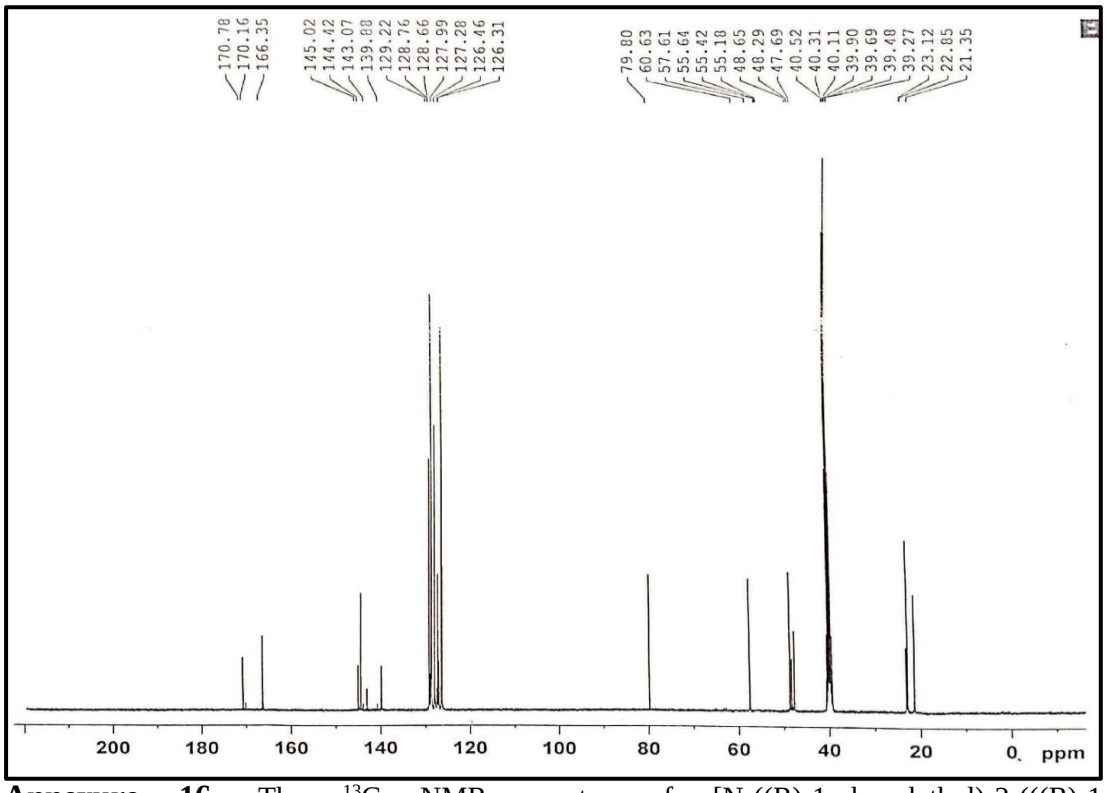

Annexure 16. The ^{13}C NMR spectra of [N-((R)-1-phenylethyl)-2-(((R)-1-phenylethyl)amino)acetamide] *R*,*R*-**3**.

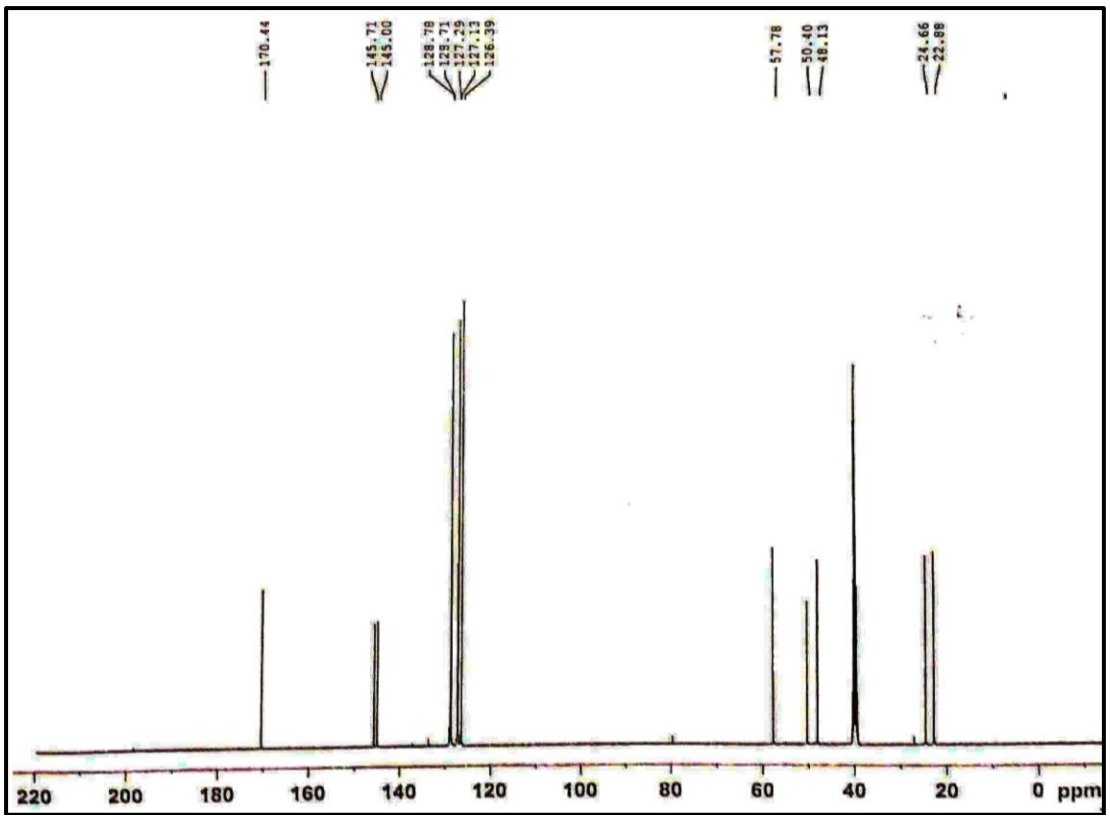

Annexure 17. The ^{13}C NMR spectra of [N-((S)-1-phenylethyl)-2-(((R)-1-phenylethyl)amino) acetamide] *S*,*R*-**4**.

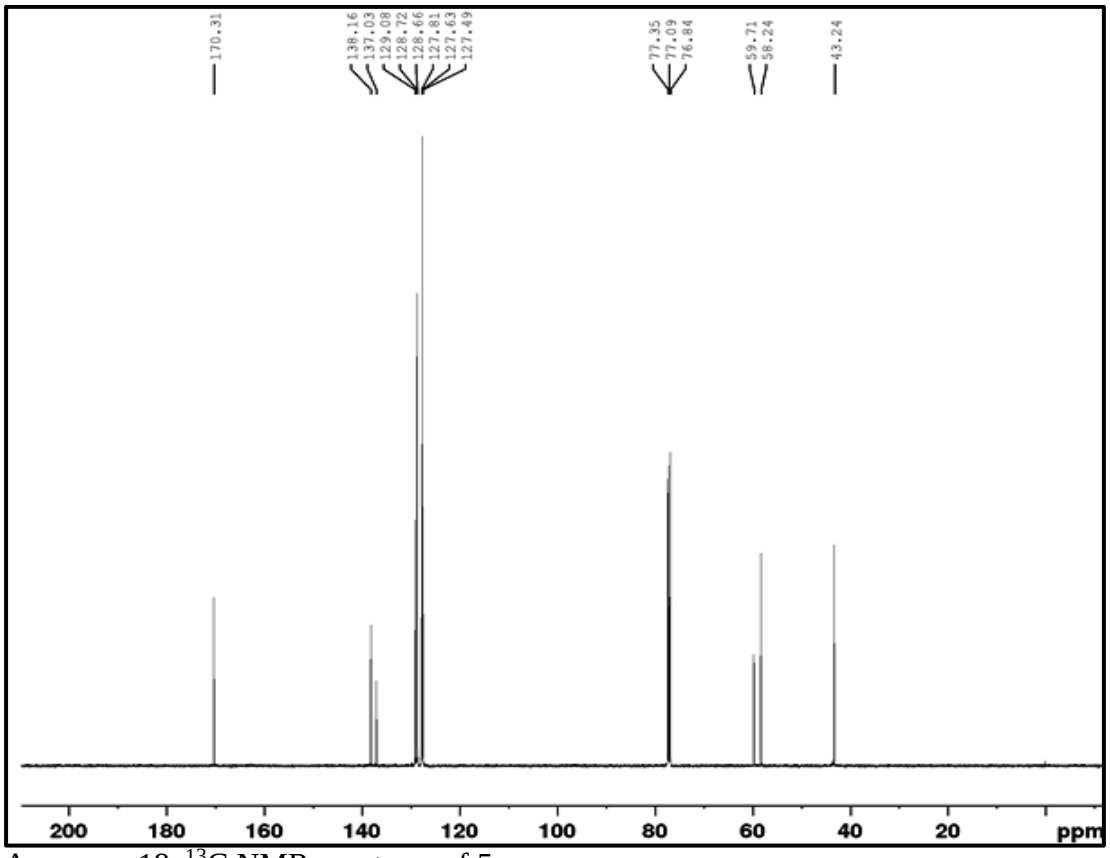

Annexure 18. ^{13}C NMR spectrum of 5.

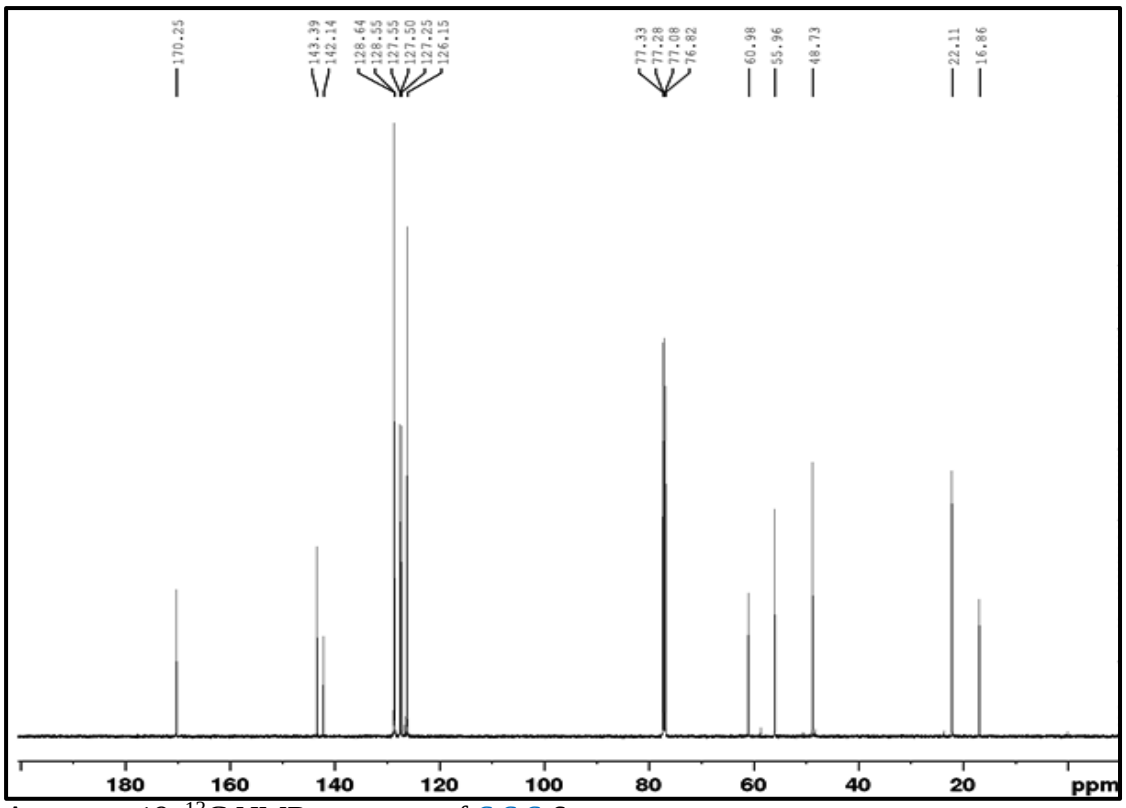

Annexure 19. ^{13}C NMR spectrum of *S,S,S*-**6**.

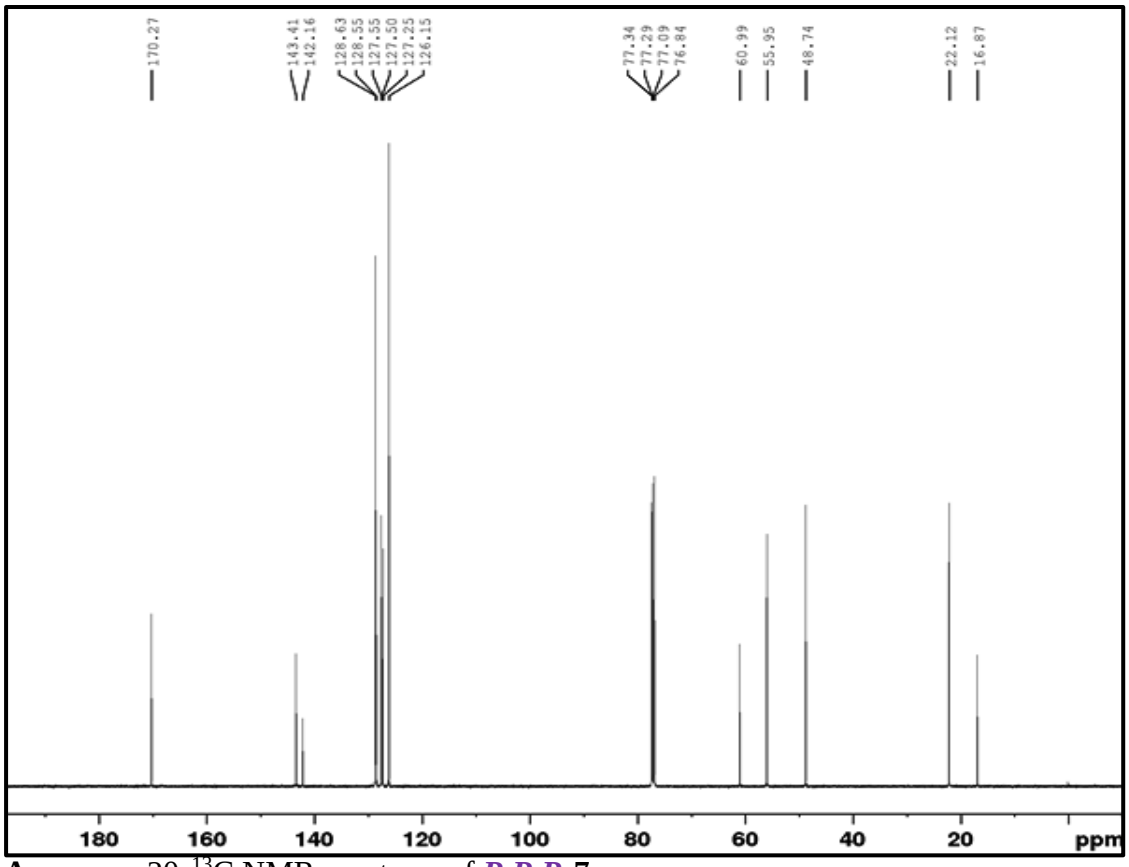

Annexure 20. ^{13}C NMR spectrum of ***R,R,R*-7**.

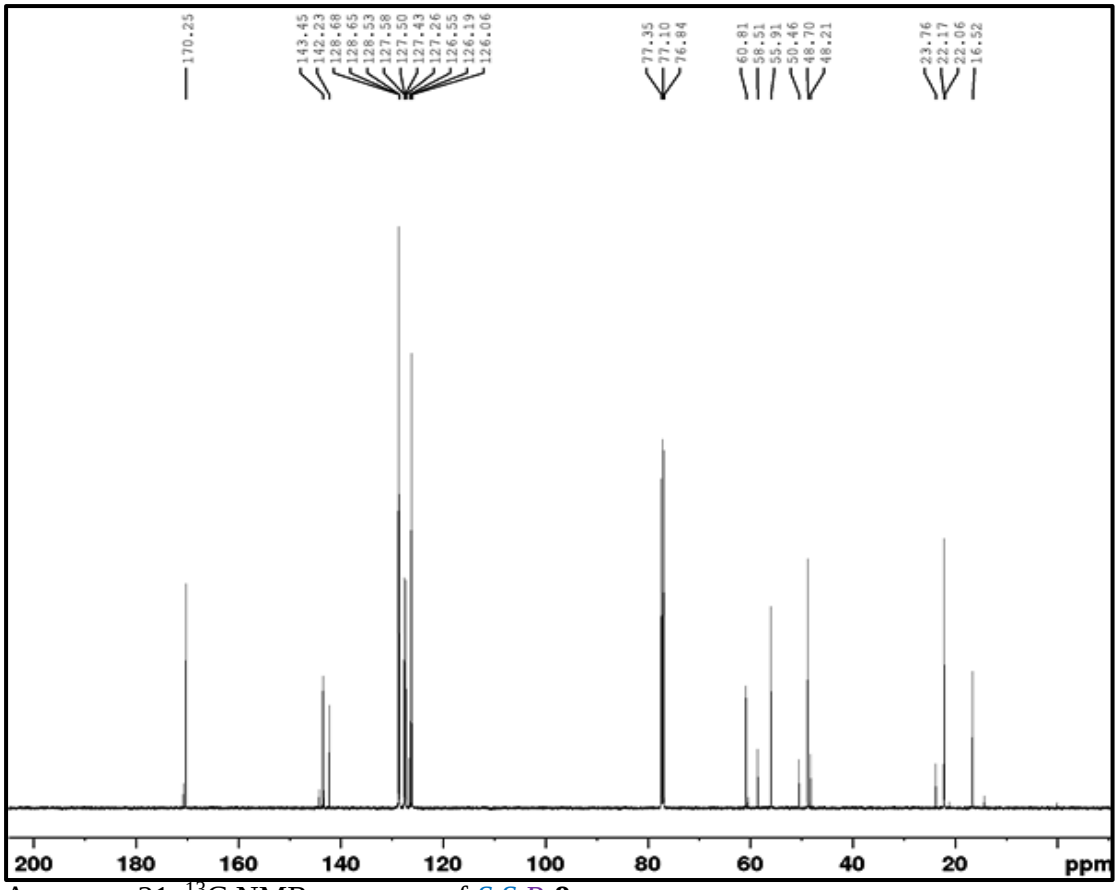

Annexure 21. ^{13}C NMR spectrum of *S,S,R*-**8**.

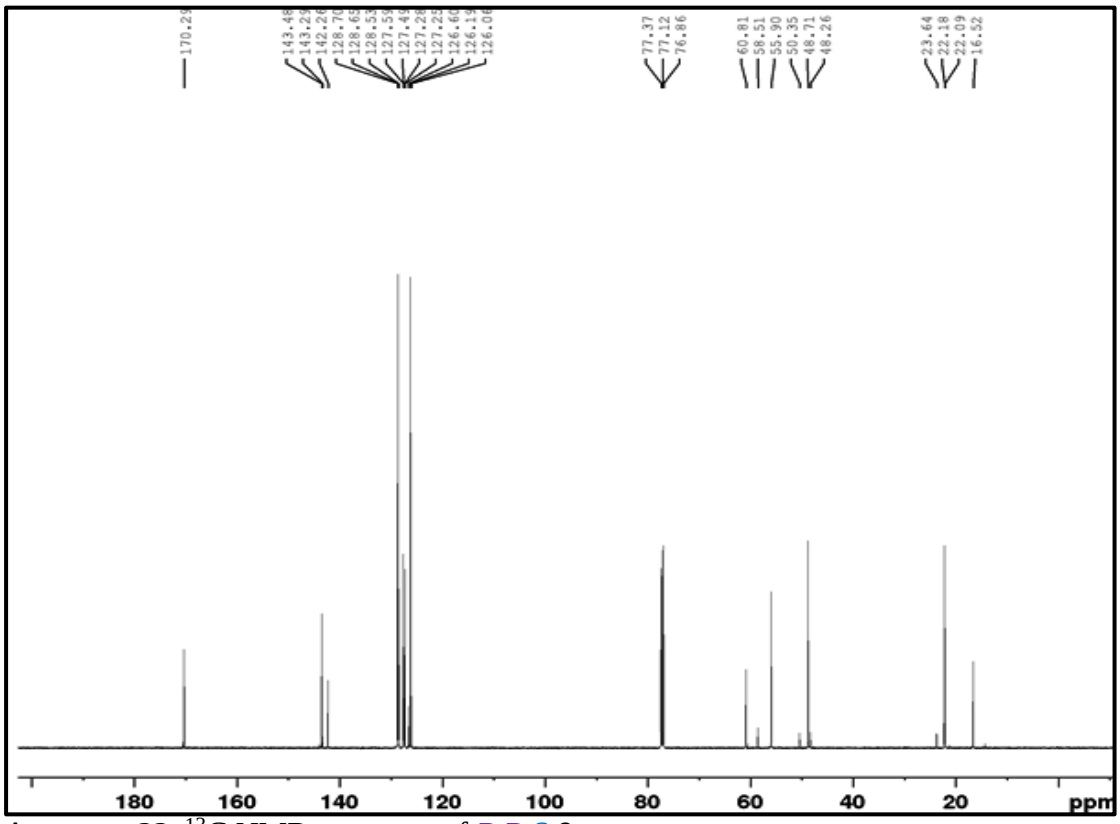

Annexure 22. ^{13}C NMR spectrum of *R,R,S*-**9**.

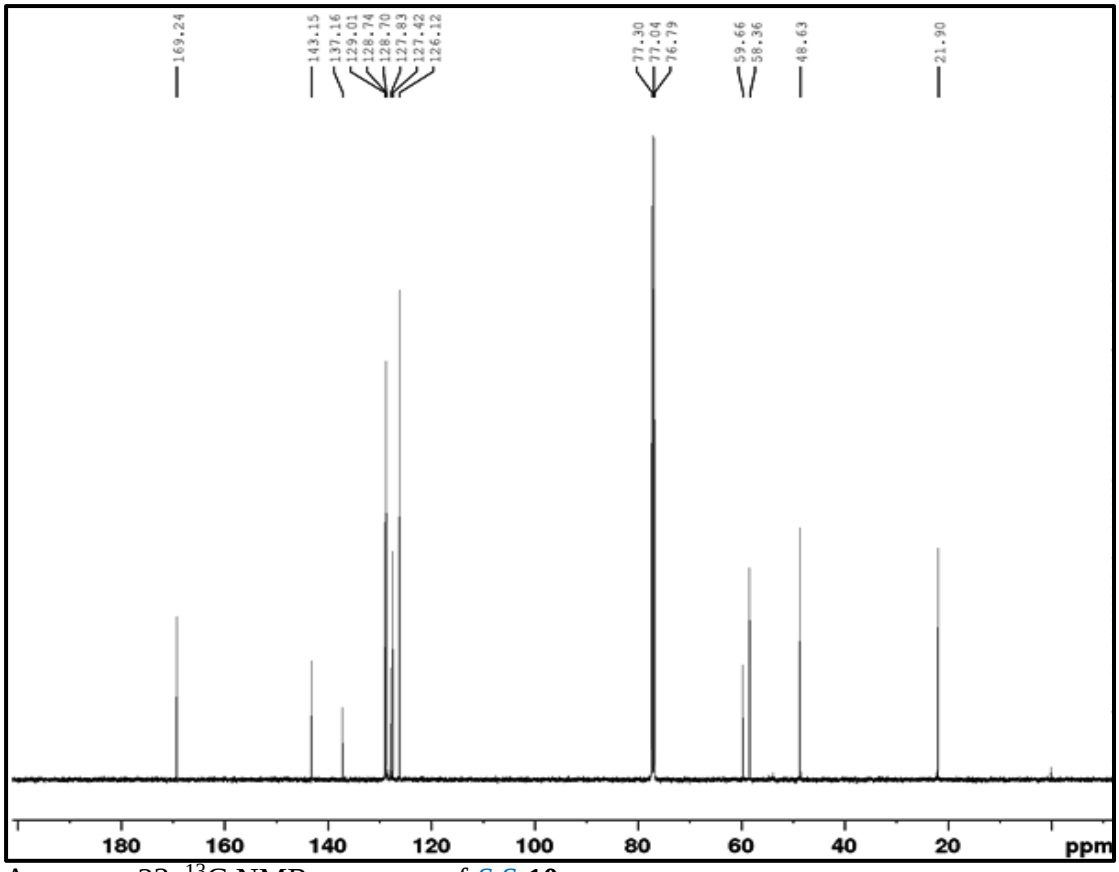

Annexure 23. ^{13}C NMR spectrum of *S,S*-**10**.

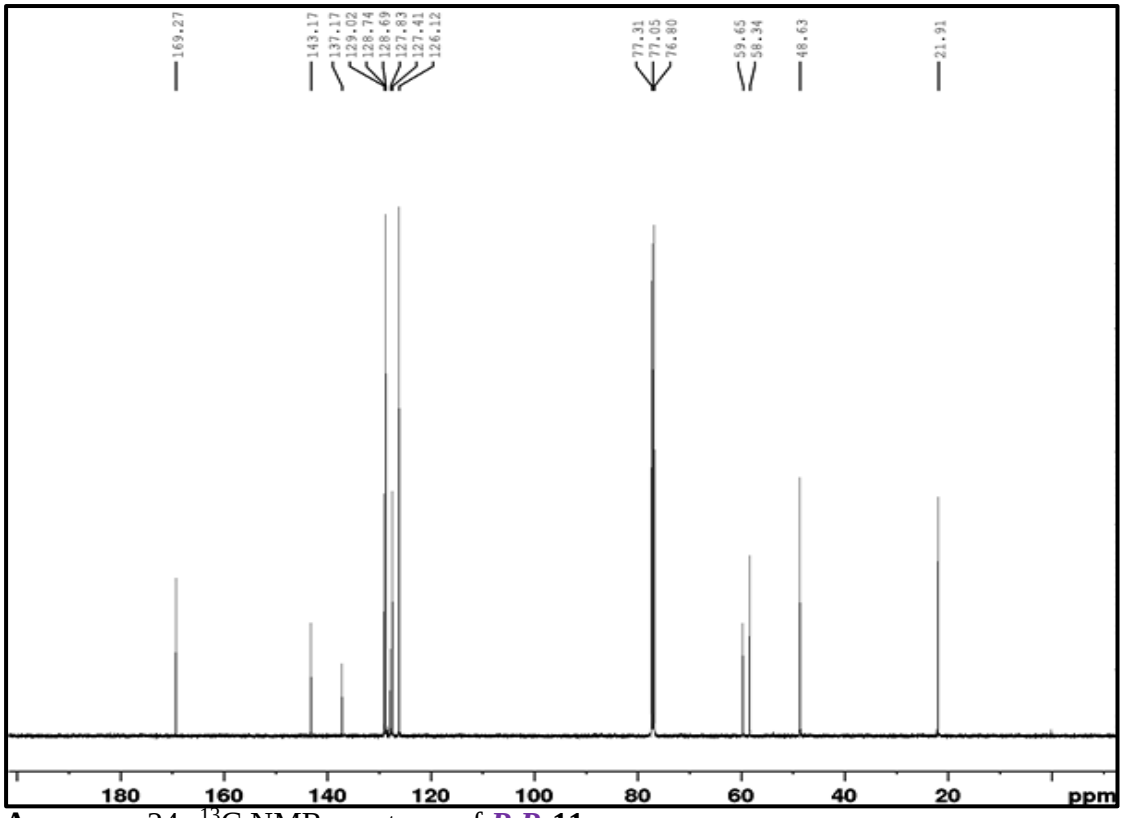

Annexure 24. ^{13}C NMR spectrum of ***R,R*-11**.

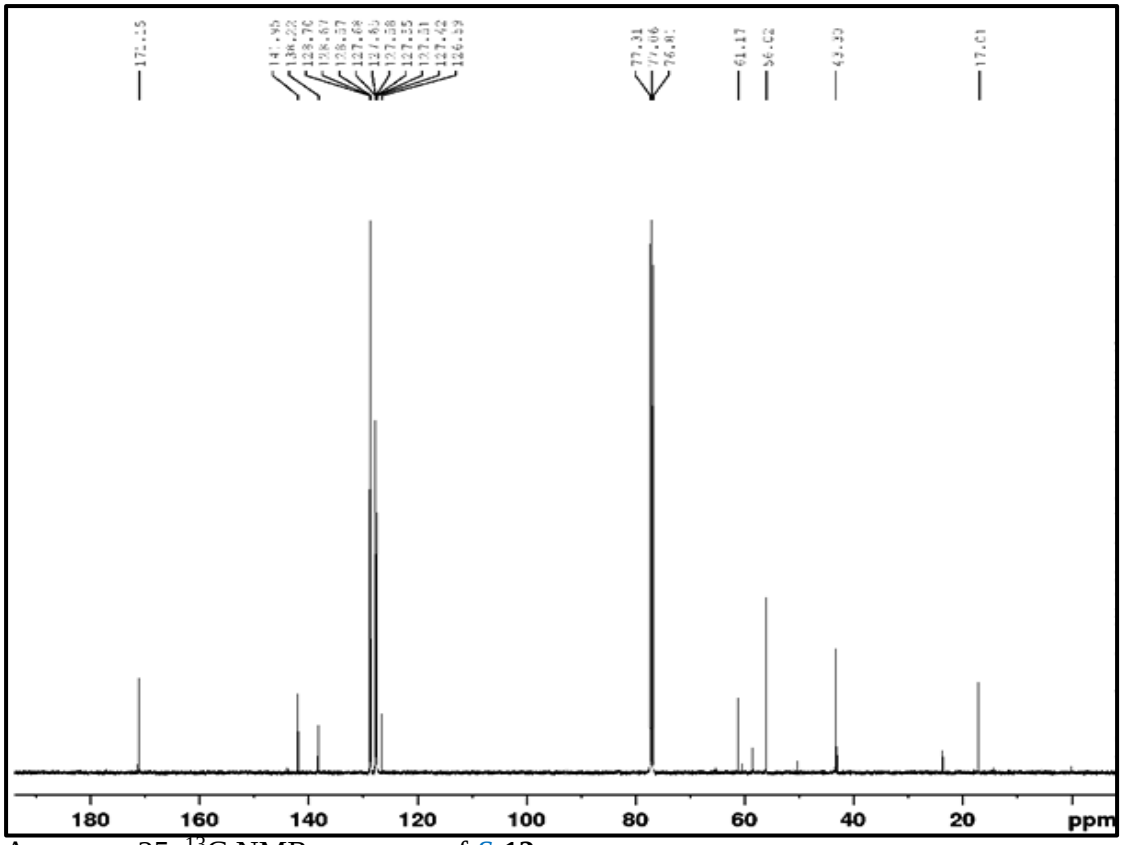

Annexure 25. ^{13}C NMR spectrum of *S*-**12**.

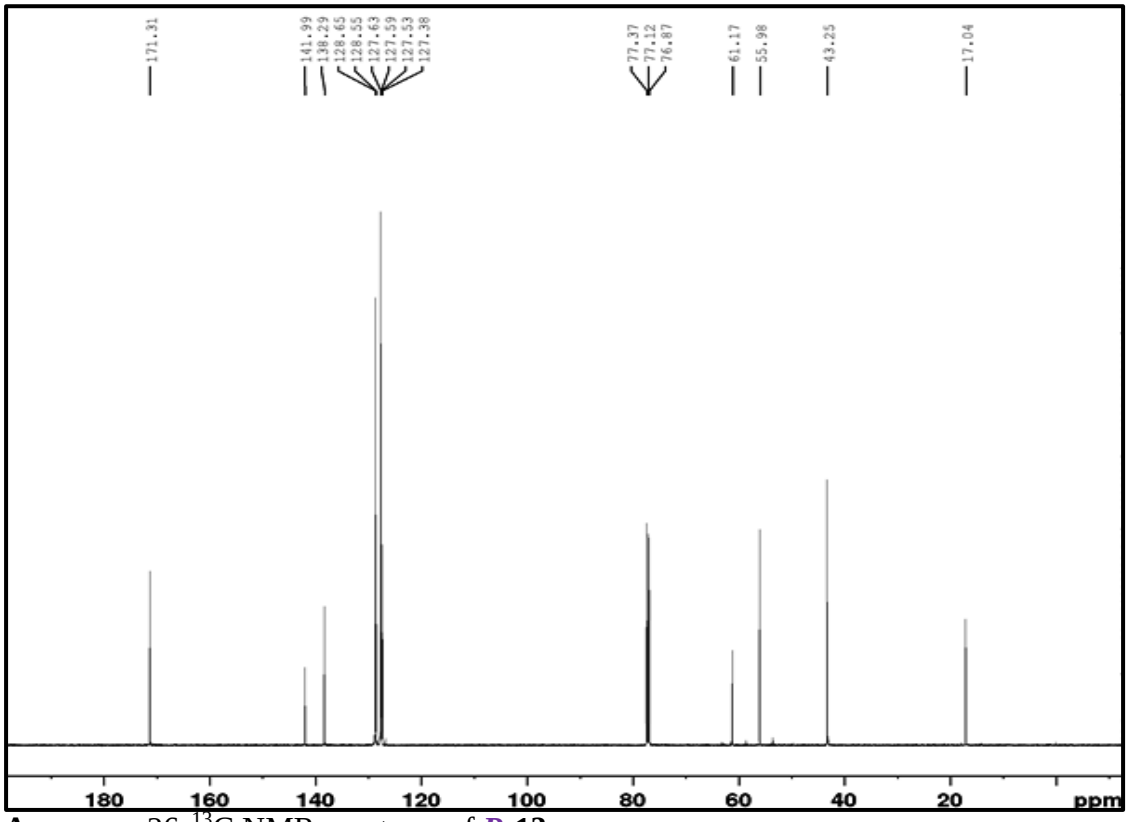

Annexure 26. ^{13}C NMR spectrum of ***R*-13**.

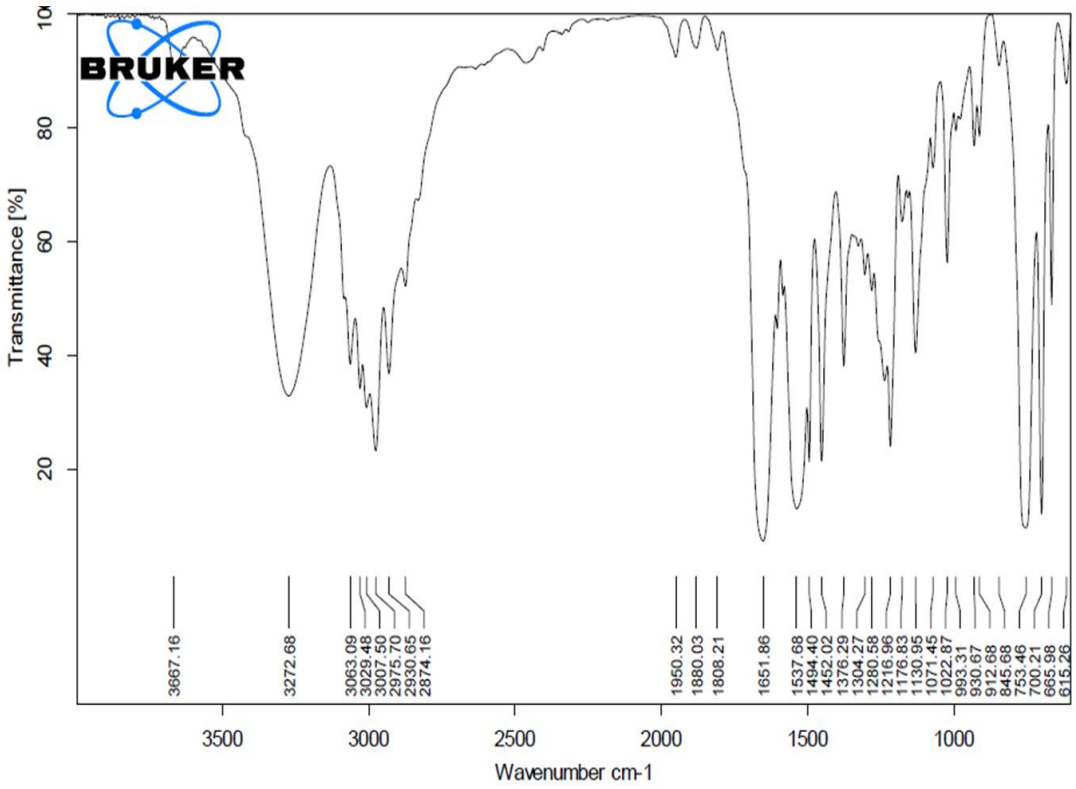

Annexure 27. The IR spectra of 1 [N-((S)-1-phenylethyl)-2-(((S)-1-phenylethyl)amino)acetamide] *S*,*S*-**1**.

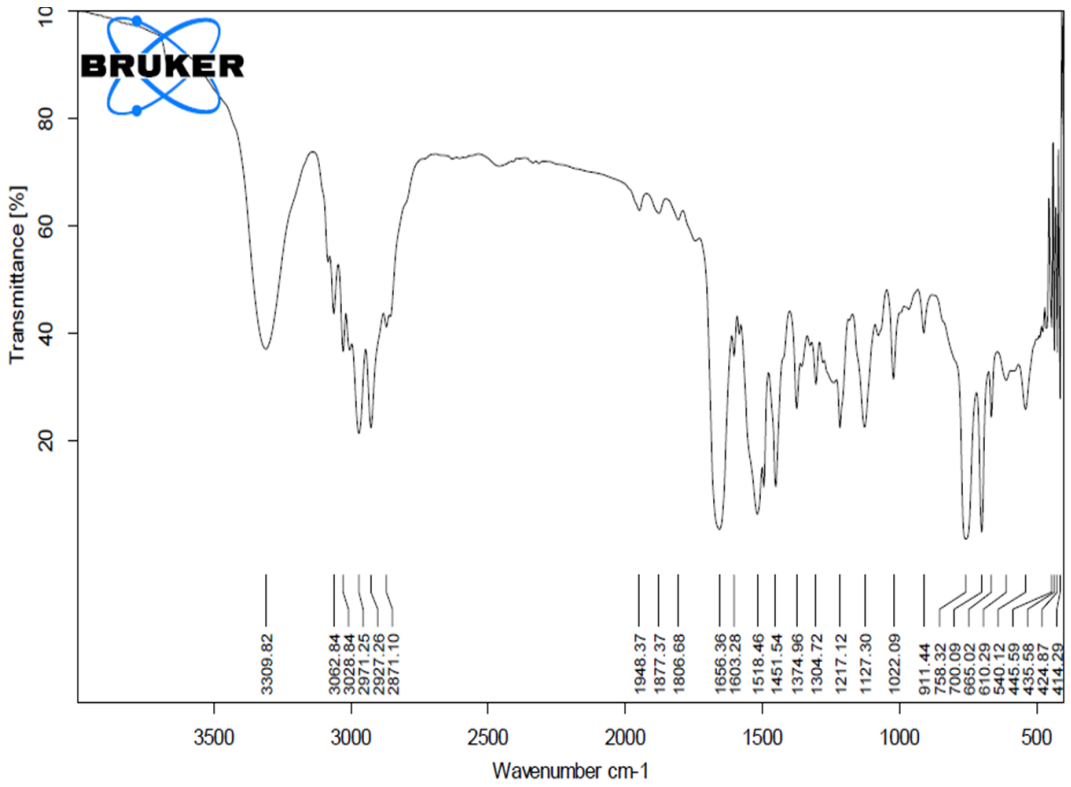

Annexure 28. The IR spectra of 2 [N-((R)-1-phenylethyl)-2-(((S)-1-phenylethyl)amino)acetamide] *R*,*S*-**2**.

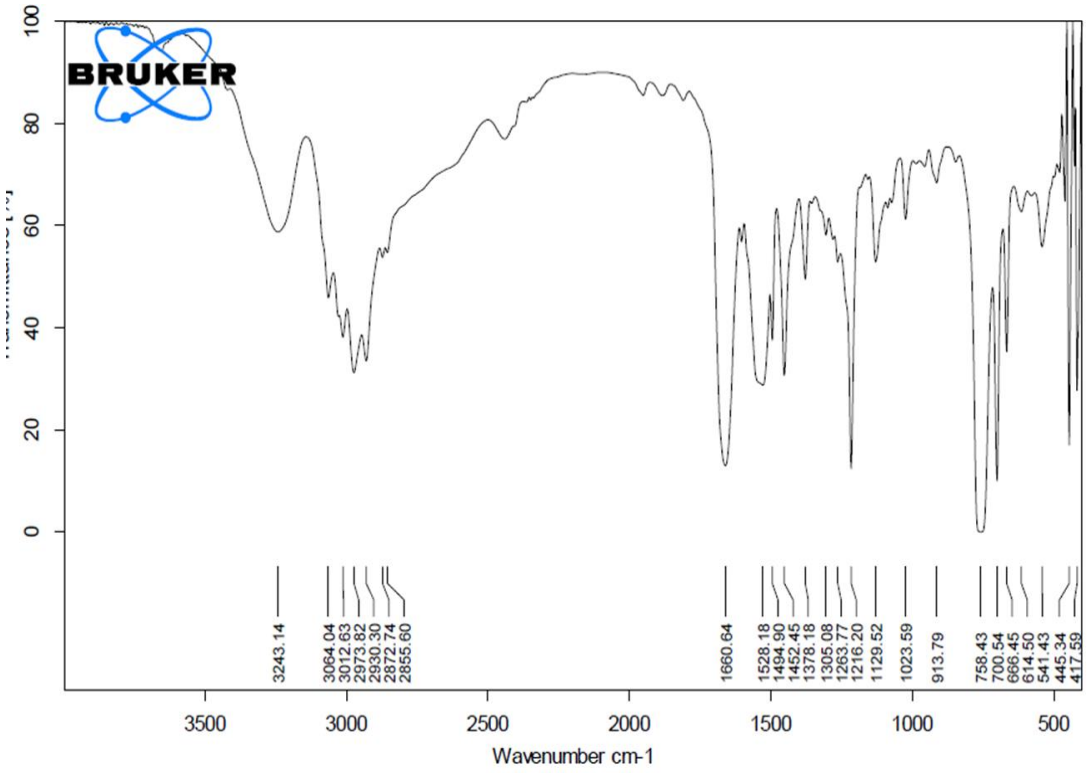

Annexure 29. The IR spectra of 3 [N-((R)-1-phenylethyl)-2-(((R)-1-phenylethyl)amino)acetamide] *R*,*R*-**3.**

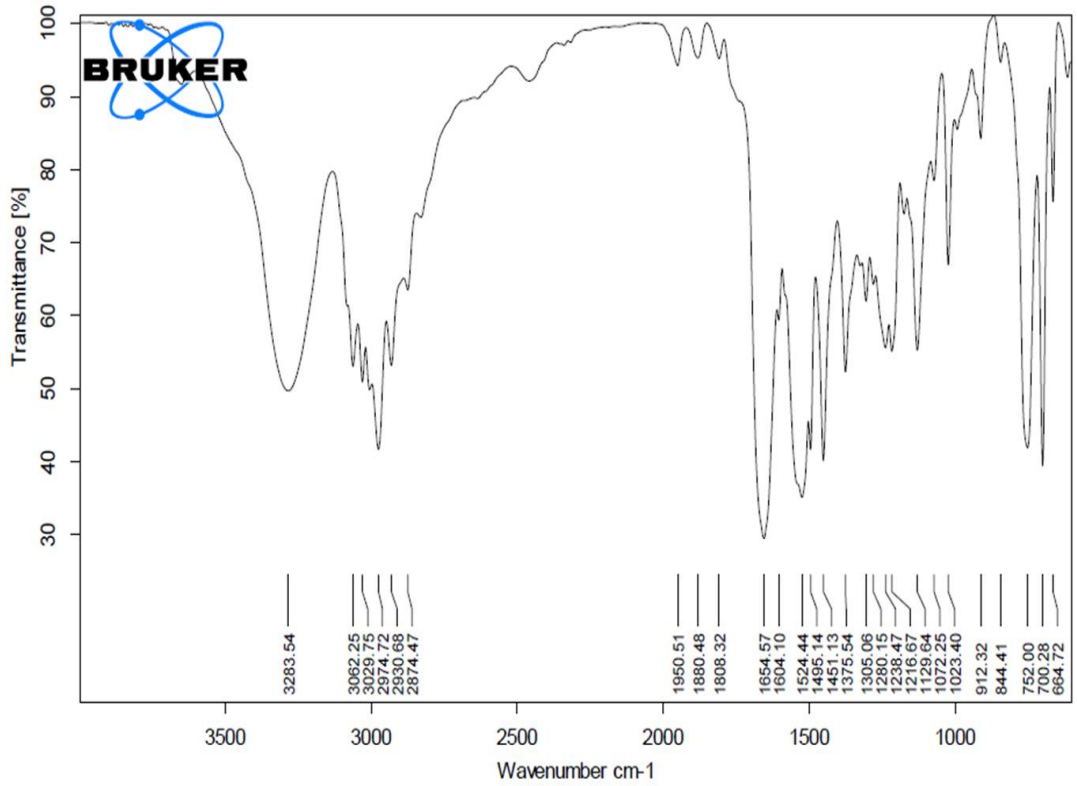

Annexure 30. The IR spectra of 4 [N-((S)-1-phenylethyl)-2-(((R)-1-phenylethyl)amino)acetamide] *S*,*R*-**4.**

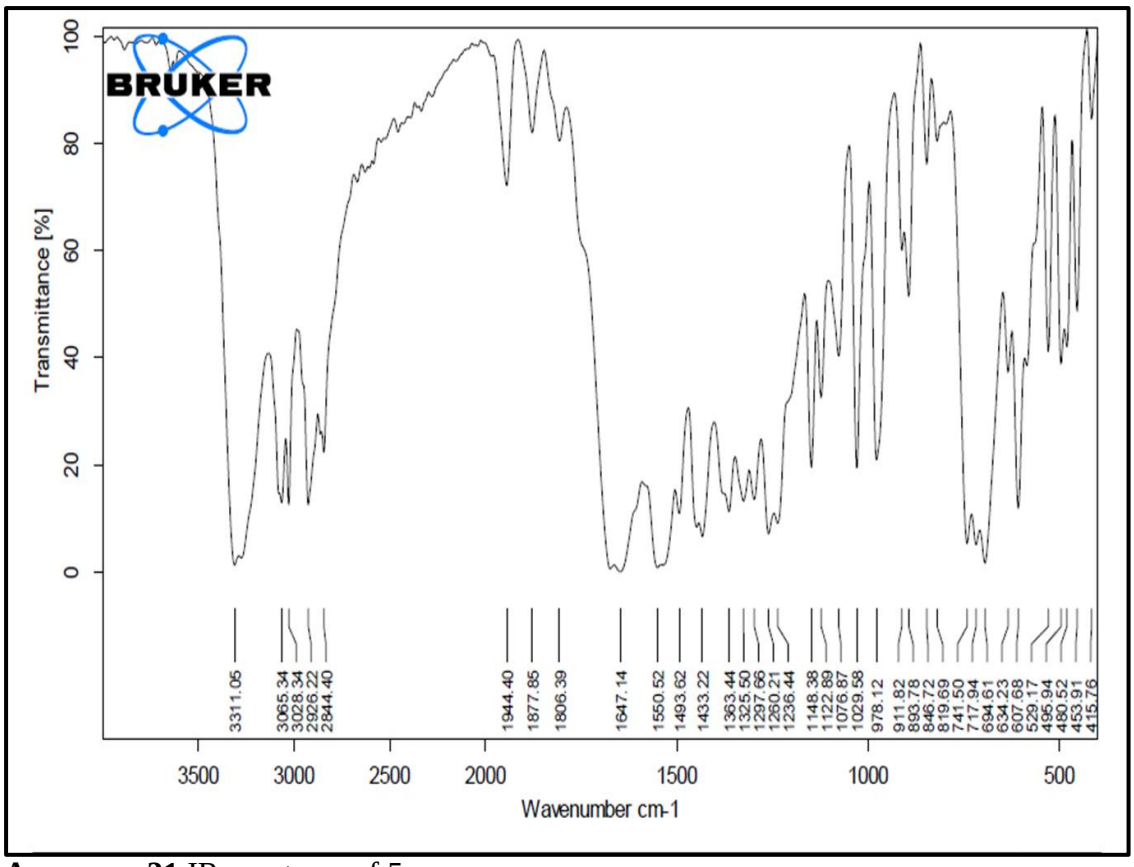

Annexure 31.IR spectrum of 5.

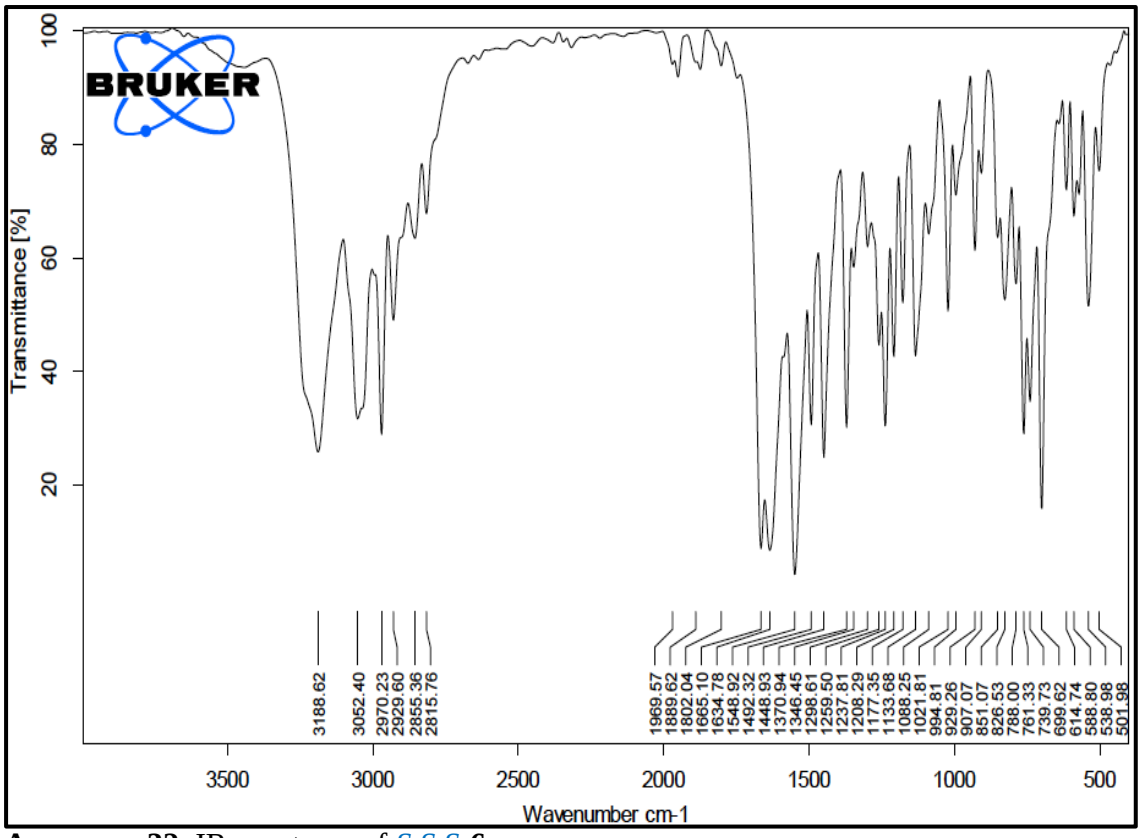

Annexure 32. IR spectrum of *S,S,S*-**6**.

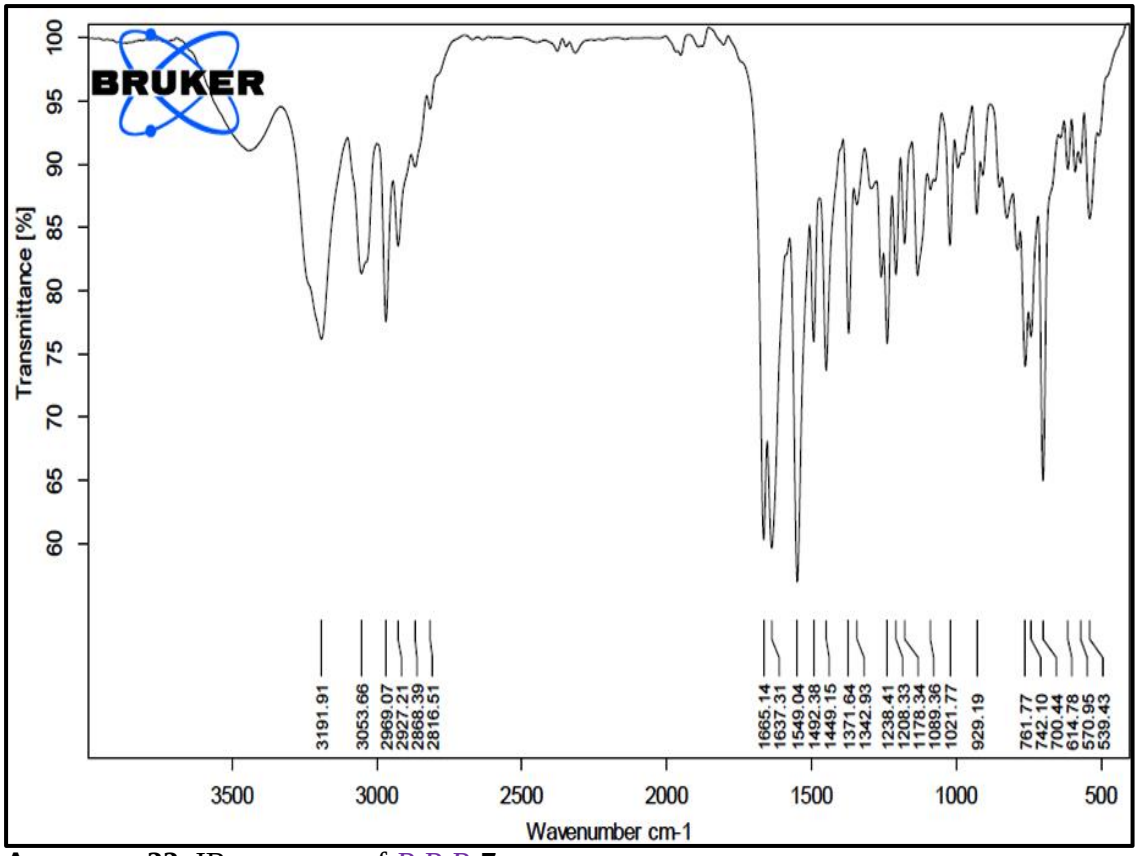

Annexure 33. IR spectrum of *R,R,R*-**7**.

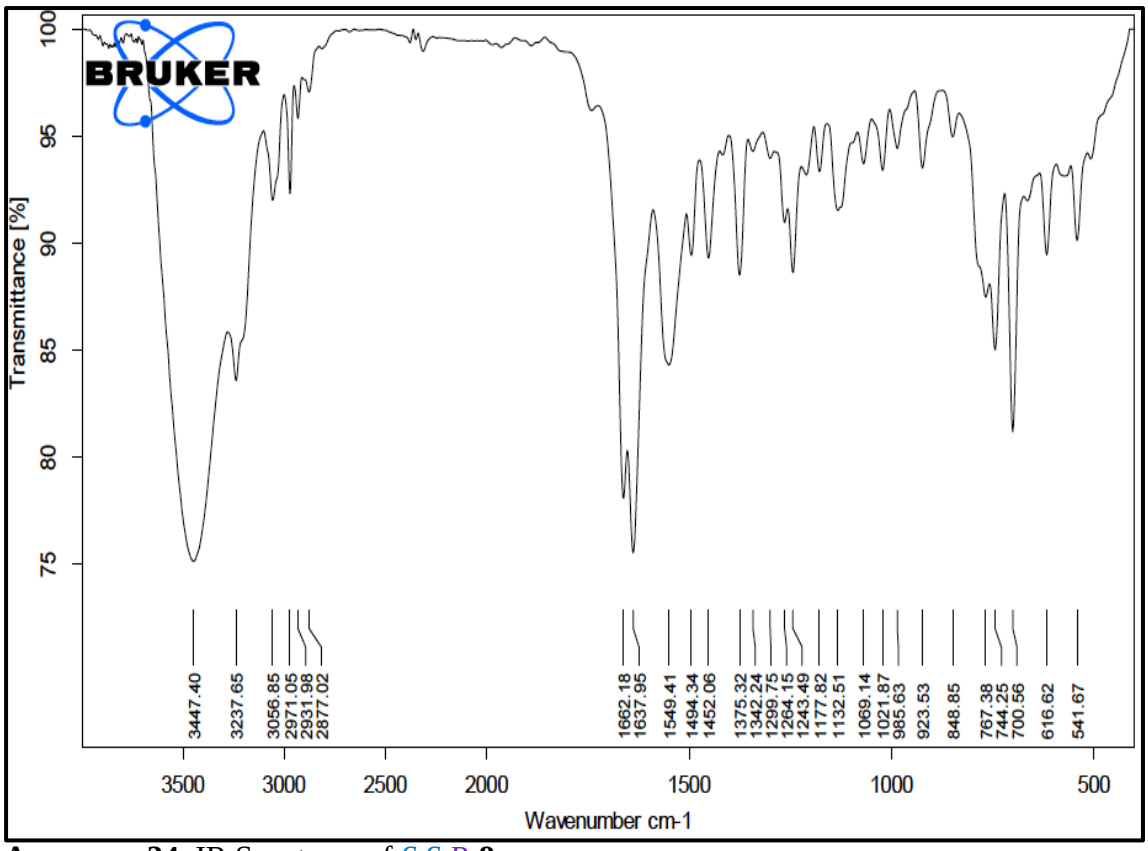

Annexure 34. IR Spectrum of *S,S,R*-**8**.

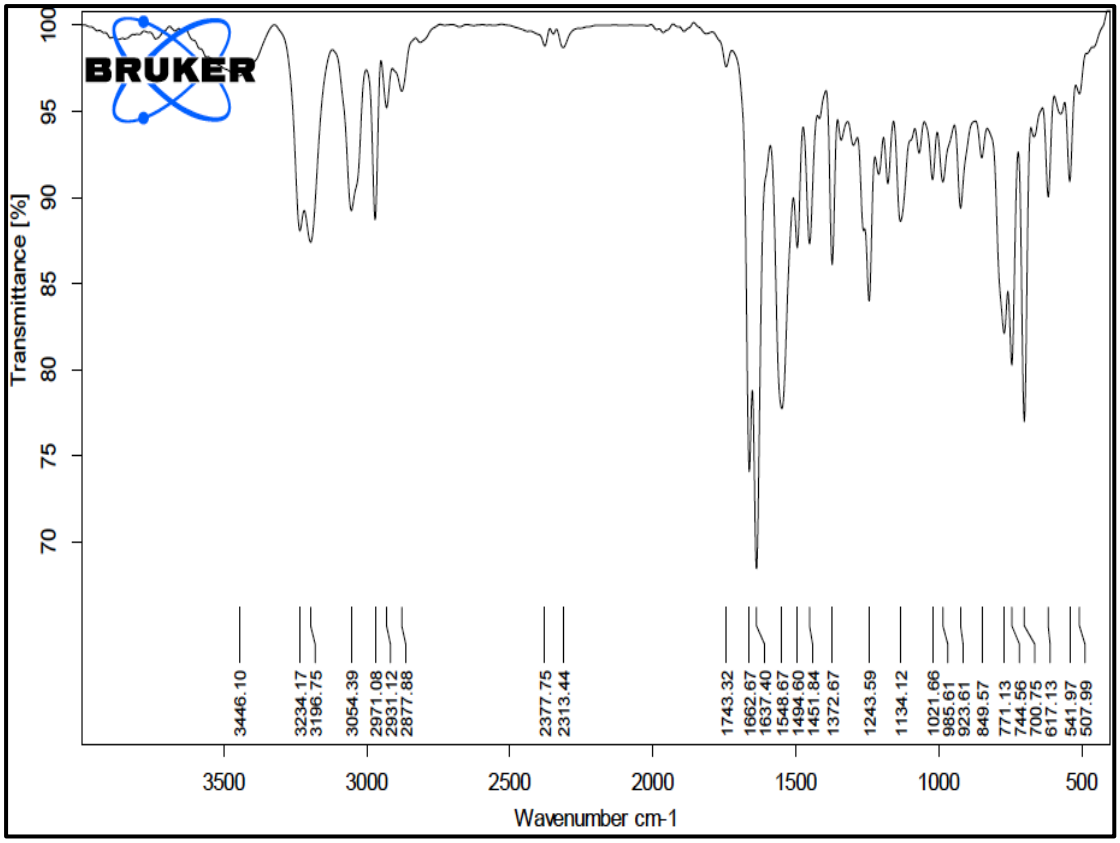

Annexure 35. IR Spectrum of *R*,*R*,*S*-**9**.

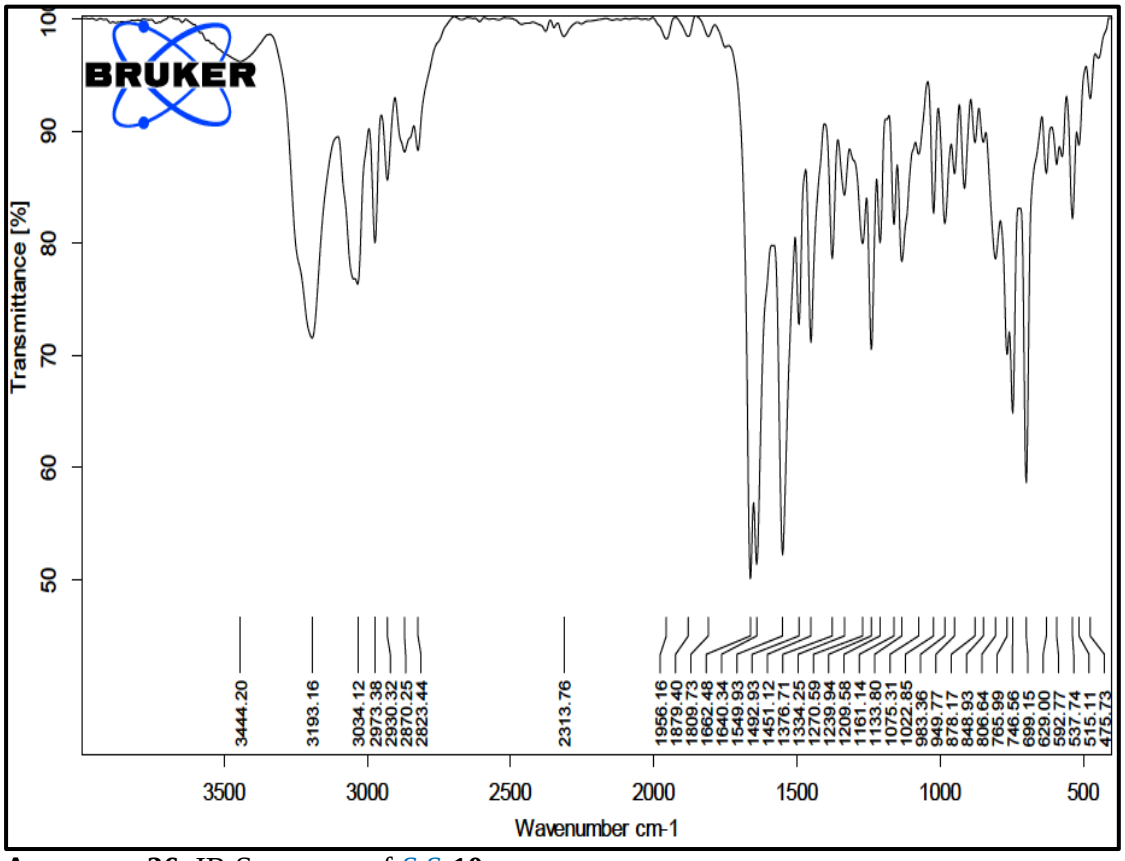

Annexure 36. IR Spectrum of *S*,*S*-**10**.

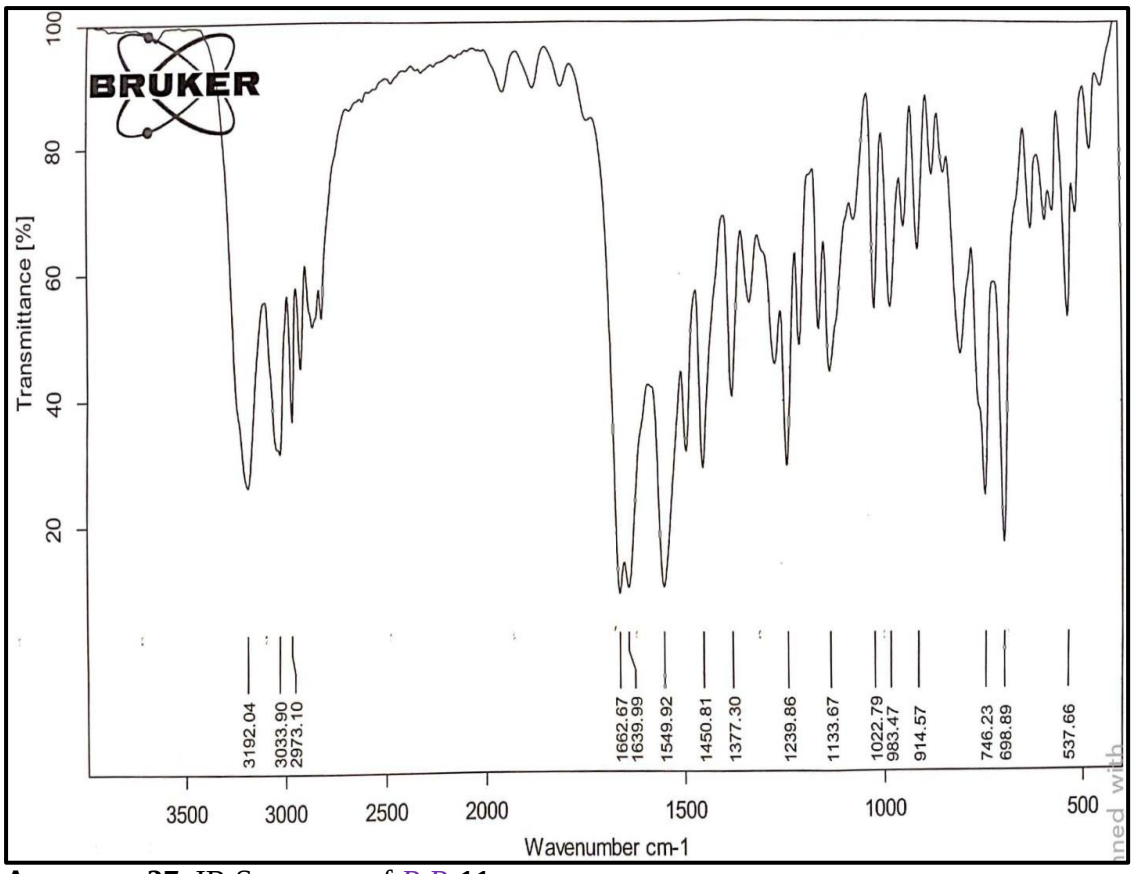

Annexure 37. IR Spectrum of *R,R*-**11**.

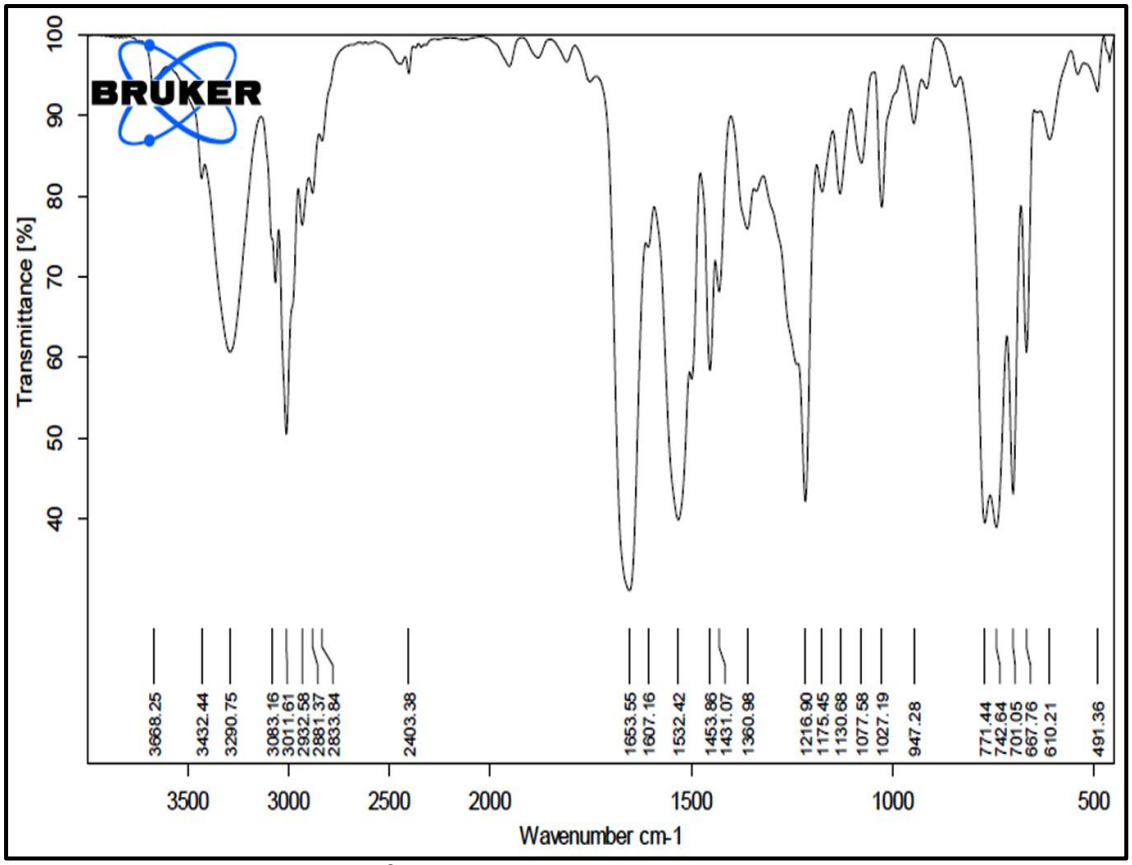

Annexure 38. IR Spectrum of *S*-**12**.

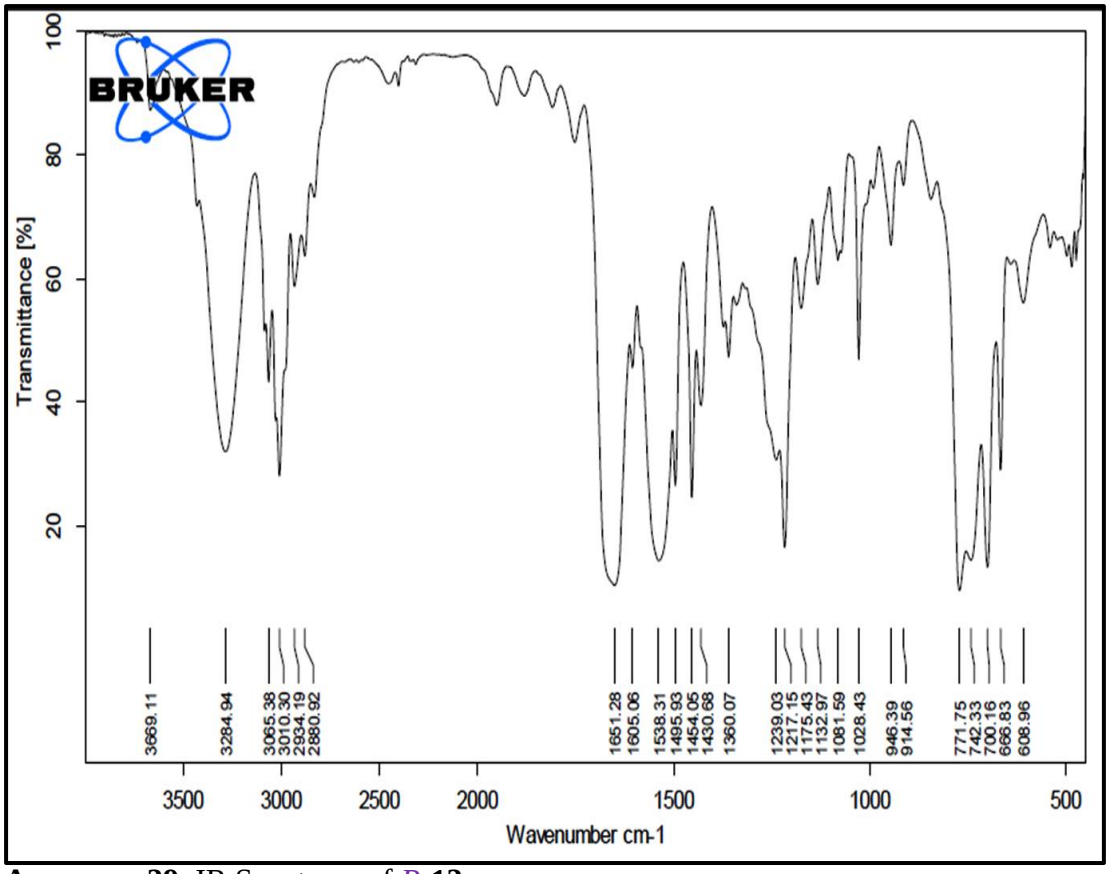

Annexure 39. IR Spectrum of *R*-**13**.